Pacific Journal of Mathematics

SYMMETRIC SURFACES OF CONSTANT MEAN CURVATURE IN $\mathbb{S}^3$

RYAN HYND, SUNG-HO PARK AND JOHN MCCUAN

Volume 241 No. 1 May 2009

PACIFIC JOURNAL OF MATHEMATICS
Vol. 241, No. 1, 2009

SYMMETRIC SURFACES OF CONSTANT MEAN CURVATURE IN $\mathbb{S}^3$

RYAN HYND, SUNG-HO PARK AND JOHN MCCUAN

We introduce two notions of symmetry for surfaces in $\mathbb{S}^3$. The first, special spherical symmetry, generalizes the notion of rotational symmetry, and we classify all complete surfaces of constant mean curvature having this symmetry. These surfaces turn out to also be rotationally symmetric, so our characterization answers a question first posed by Hsiang in 1982 and also considered by several authors since. From this point of view, these are the Delaunay surfaces of $\mathbb{S}^3$.

Our second notion of symmetry, spherical symmetry, is a substantial, and we believe important, technical generalization of special spherical symmetry. We classify all compact surfaces of constant mean curvature having this symmetry. We show in particular that the only compact embedded minimal surfaces possessing this kind of symmetry are the great spheres and the Clifford torus.

We derive from our classification theorem a special case of Lawson's conjecture that the only embedded minimal torus in $\mathbb{S}^3$ is the Clifford torus.

Introduction

We consider surfaces in the three-dimensional sphere $\mathbb{S}^3 = \{\mathbf{x} \in \mathbb{R}^4 : |\boldsymbol{x}| = 1\}$. Perhaps the simplest notion of symmetry for surfaces in $\mathbb{S}^3$ is that of rotational symmetry, as exemplified by the Clifford torus

$$\mathscr{C} = \{(x, y, z, w) \in \mathbb{R}^4 : x^2 + y^2 = 1/2 = z^2 + w^2\}.$$

It is usual to explain the symmetry of such a surface by saying it is invariant under an $\mathbb{S}^1$ action that fixes a geodesic. We will take a somewhat different approach

MSC2000: 53A10.

Keywords: Delaunay surfaces, constant mean curvature, Willmore surfaces, Clifford torus, minimal surfaces, submanifolds in space forms, Lawson's conjecture.

Hynd was supported in part by the Georgia Tech School of Mathematics VIGRE program and a Georgia Tech Summer Research Assistantship. Park was supported by the Postdoctoral Fellowship Program of the Korean Science & Engineering Foundation (KOSEF). McCuan was supported in part by NSF grant DMS-0103848, and portions of the work were completed at the Max-Planck-Institut für Mathematik in den Naturwissenschaften.

suggested by the decomposition of rotational symmetry into some sufficient number of invariances under reflection maps. Such a decomposition was first used by Alexandrov [1962] and modified in the direction of our interest in [Wente 1980] and [McCuan 1997]. Each of these papers consider surfaces in $\mathbb{R}^3$, and though the symmetry conditions considered here are described directly in $\mathbb{S}^3$ without reference to particular coordinates, we find it easiest to think about and describe these results in terms of stereographic projections into $\mathbb{R}^3$ of the geometric objects involved.

The surface $\mathscr{C}$ mentioned above stereographically projects to the anchor ring

$$\left\{(x, y, z) \in \mathbb{R}^3 : \left(\sqrt{x^2 + y^2} - \sqrt{2}\right)^2 + z^2 = 1\right\},$$

which is rotationally symmetric in $\mathbb{R}^3$. The anchor ring is invariant under the orientation-reversing transformation of reflection through each vertical plane containing the z-axis. If we apply a preliminary rotation R of $\mathbb{S}^3$ to obtain the congruent torus $R(\mathscr{C})$, the stereographic projection of $R(\mathscr{C})$ will not, in general, be invariant under the orientation-preserving isometry of rotation in $\mathbb{R}^3$. Properly generalized, however, invariance under reflections (Kelvin transforms) will be preserved.

Our first symmetry condition, *special spherical symmetry*, is more general than, but includes, the usual condition of being invariant under an $\mathbb{S}^1$ action that fixes a geodesic. Roughly speaking, the stereographic projection must be invariant under a continuous one-parameter family of reflections (that is, Kelvin transforms) through spheres, and these reflections must fit together in a nice way, that is, satisfy a coherence condition. The case of rotational symmetry (of Alexandrov and Wente and the standard projection of the Clifford torus) mentioned above appears as a kind of degenerate case in which each of the spheres is a plane, and the coherence condition requires that the planes all contain a common line. In the more general case, it is required that the spheres of symmetry all contain a common circle.

Notice also that there are certainly surfaces in $\mathbb{S}^3$ with stereographic projection rotationally symmetric in $\mathbb{R}^3$ but that do not satisfy the usual definition of rotational symmetry in $\mathbb{S}^3$. The fact that our new notions of symmetry do not depend on isometries of $\mathbb{S}^3$ is one of the reasons that they are more general and one of the main reasons they are of interest.

In Section 2 we classify all complete, connected constant mean curvature surfaces having this symmetry; see Theorem 1 below. The classified surfaces are parameterized explicitly in terms of elliptic integrals, and we can determine completely the topology, and compactness in particular, of each surface.

Next, we introduce a more general symmetry condition, *spherical symmetry*, in which continuity of the one-parameter family of reflections is relaxed and the

coherence condition is partially relaxed. More precisely, in the stereographic projection, the symmetry spheres are not required to contain a common circle, but their Euclidean centers are required to be points on a Euclidean line.

In Section 3 we show that all compact surfaces with spherical symmetry actually posses special spherical symmetry; see Theorem 2. This classification restricted to those surfaces that are embedded, compact and minimal gives a special case of Lawson's conjecture [Yau 1982, Problem 97]:

Theorem. *The Clifford torus is the only embedded minimal torus with spherical symmetry.*

A somewhat analogous result under very different symmetry assumptions was obtained by Ros [1995]. The referee brought to our attention the very beautiful paper of Kilian and Schmidt [2008], which gives a much more extensive discussion of Lawson's conjecture than found here and proves the result under the assumption that the torus has finite type.

The classification of complete constant mean curvature surfaces with spherical symmetry remains open. We suspect there are no new surfaces in this broader class, but we use compactness very strongly and cannot make that assertion with any confidence.

Ultimately, the conditions of special spherical symmetry and spherical symmetry each rely on invariance of the image of the surface considered as an immersion into $\mathbb{S}^3$ from an abstract Riemannian manifold. For this reason, we must make preliminary arguments in Section 1 to obtain an explicit local parameterization on a domain in $\mathbb{R}^2$ whose dependent variables will satisfy explicit differential equations. The existence of such parameterizations has been, as far as we can tell, simply assumed in the literature. Our basic parameterization result, Theorem 4, should naturally generalize to apply in other contexts. Once a parameterization is obtained, stereographic projection plays a key role again in providing a crucial change of variables through which the equation of constant mean curvature takes a form amenable to explicit integration.

Rossman and Sultana [2007; 2008] have recently considered classification questions similar to those considered here. The particular coordinates we have chosen are crucial to the latter developments of the paper and have other advantages as well, including making obvious the identification of these surfaces with the surfaces of Delaunay and permitting easy access to explicit integral representation. Both of these topics will be discussed further below.

0.1. ***Reflection and special spherical symmetry.*** We now describe the notion of *generalized* (or spherical) *reflection maps*, on which our symmetry conditions are based. There are two kinds of generalized reflection maps $f : \mathbb{S}^3 \to \mathbb{S}^3$. The first is

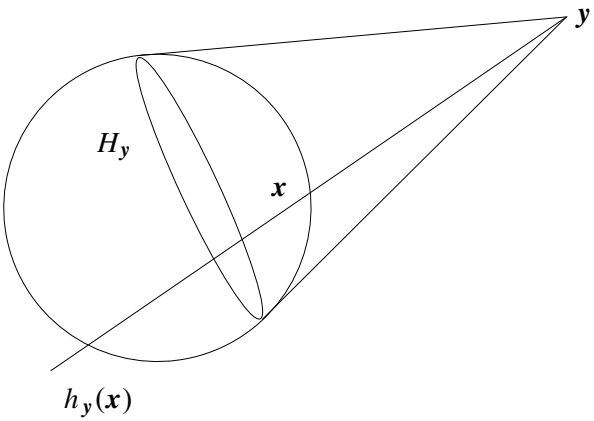

Figure 1. Cone point reflection.

the restriction to $\mathbb{S}^3$ of appropriate reflections of $\mathbb{R}^4$. To be precise, given $\boldsymbol{n} \in \mathbb{S}^3$,

$$g_{\boldsymbol{n}} : \mathbb{S}^3 \to \mathbb{S}^3, \quad \boldsymbol{x} \mapsto \boldsymbol{x} - 2(\boldsymbol{x} \cdot \boldsymbol{n})\boldsymbol{n}$$

is the restriction to $\mathbb{S}^3$ of the reflection through the (hyper)plane $\{\boldsymbol{x} \in \mathbb{R}^4 : \boldsymbol{x} \cdot \boldsymbol{n} = 0\}$. The intersection of this plane with $\mathbb{S}^3$ is the great sphere $G_{\boldsymbol{n}} = \{\boldsymbol{x} \in \mathbb{S}^3 : \boldsymbol{x} \cdot \boldsymbol{n} = 0\}$; we will call such maps great sphere reflections, and they may be identified either by the corresponding great sphere $G_{\boldsymbol{n}}$ or a corresponding normal $\boldsymbol{n}$ (determined up to a sign). The great sphere $G_{\boldsymbol{n}}$ is also called the *symmetry sphere* of $g_{\boldsymbol{n}}$.

The second kind of map we wish to consider is determined by a point $\boldsymbol{y} \in \mathbb{R}^4$ with $|\boldsymbol{y}| > 1$. Each is an orientation-reversing diffeomorphism

$$h_{\boldsymbol{y}} : \mathbb{S}^3 \to \mathbb{S}^3, \quad \boldsymbol{x} \mapsto \boldsymbol{y} + (|\boldsymbol{y}|^2 - 1)\frac{\boldsymbol{x} - \boldsymbol{y}}{|\boldsymbol{x} - \boldsymbol{y}|^2}.$$

The formula for $h_{\boldsymbol{y}}$ also has a simple geometric interpretation. If ℓ is the line through $\boldsymbol{y}$ and $\boldsymbol{x}$, then $\ell \cap \mathbb{S}^3 = \{\boldsymbol{y}, h_{\boldsymbol{y}}(\boldsymbol{x})\}$. The fixed point set of $h_{\boldsymbol{y}}$ is the nondegenerate sphere

$$H_{\boldsymbol{y}} = \{\boldsymbol{x} \in \mathbb{S}^3 : \boldsymbol{x} \cdot \boldsymbol{y} = 1\},$$

which we call the symmetry sphere of $h_{\boldsymbol{y}}$. Note that if an observer is located at $\boldsymbol{y}$, then $H_{\boldsymbol{y}}$ appears as the horizon on $\mathbb{S}^3$; see Figure 1. Accordingly, we refer to $h_{\boldsymbol{y}}$ as the cone point reflection based at the *cone point* $\boldsymbol{y} \in \mathbb{R}^4 \setminus \overline{B_1(0)}$; the map $h_{\boldsymbol{y}}$ may be identified uniquely by either its horizon sphere $H_{\boldsymbol{y}}$ or its cone point $\boldsymbol{y}$.

Definition 1 (special spherical symmetry). A set $\mathcal{S} \subset \mathbb{S}^3$ has *special spherical symmetry* if $\mathcal{S}$ is invariant under a family of generalized reflections consisting of either all the great sphere reflections $g_{\boldsymbol{n}}$ associated to the points $\boldsymbol{n}$ of a great circle in $\mathbb{S}^3$ or all the cone point reflections $h_{\boldsymbol{y}}$ associated to a line in $\mathbb{R}^4 \setminus \overline{B_1(0)}$.

0.2. ***Classification theorem.*** Our classification by Theorem 1 of constant mean curvature (CMC) surfaces with special spherical symmetry bears a strong superficial resemblance to the classification of Delaunay surfaces (rotationally symmetric constant mean curvature surfaces in $\mathbb{R}^3$). Recall that the Delaunay surfaces form a two parameter family consisting of six qualitative types: spheres, cylinders, catenoids, unduloids, nodoids, and planes. We borrow this terminology, so we briefly recall some properties of these surfaces.

The surfaces of Delaunay are often indexed by the two parameters mean curvature and neck size (the minimum distance from the meridian curve to the axis). Neck size is positive, except for the spheres and the plane. After a rigid motion, one may assume the axis of rotation is the vertical z-axis in $\mathbb{R}^3$ and that each surface has a natural parameterization of the form

$$(t, \theta) \mapsto (r\cos\theta, r\sin\theta, u), \tag{1}$$

where $t \mapsto (r(t), u(t))$ parameterizes the surface's meridian curve. Catenoids have a unique neck, that is, point on the meridian curve closest to the axis. The meridian curve of a catenoid is an embedded graph of an unbounded convex function over the entire axis of rotation. After translating the neck to $z = 0$, the meridian is even.

The unduloids and nodoids have periodic meridians. The meridian of an unduloid is an embedded graph with one positive minimum (neck), one maximum (bulge), and one inflection per closed half period, as shown in Figure 2. The nodoids have immersed meridians of nonvanishing curvature with loops toward the axis. When considered as a limit of unduloids or nodoids (neck size tending to zero), the sphere naturally arises as a "string of pearls".

Note finally that a multiple cover of the surface arises from the parameter θ in (1). The parameterization becomes singular when r vanishes, as in the case of the sphere and plane. Our classification theorem also gives a natural parameterization (2) containing a wrapping parameter ϕ and a dependent function r whose behavior is completely analogous.

Theorem 1. *The complete CMC surfaces in $\mathbb{S}^3$ with special spherical symmetry form, up to rigid motions, a-two parameter family consisting of five qualitatively different types of surfaces.*

Generating curves and parameterization. *Associated to each surface is a parametric curve $\gamma : t \mapsto (r(t), \theta(t))$ given explicitly in terms of elliptic integrals. Given the generating curve γ, a fundamental domain on the corresponding surface is parameterized by $X : \mathrm{Dom}(\gamma) \times \mathbb{R} \to \mathbb{S}^3$, where*

$$X(t, \phi) = \frac{1}{R\sqrt{r^2+1}}(R\cos\theta, R\sin\theta, r\sin\phi, R\sqrt{r^2+1} - 1) \tag{2}$$

and $R = \sqrt{r^2+1} + r\cos\phi$.

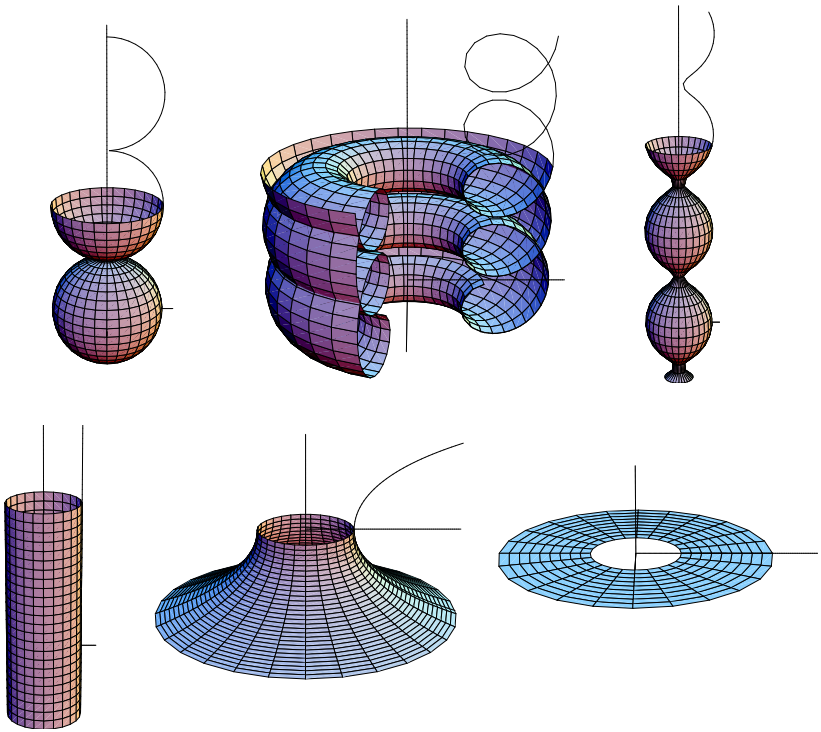

Figure 2. The Delaunay surfaces and their meridian curves and immersions: sphere, nodoid, unduloid, cylinder, catenoid, plane.

Differential equation and parameters for the space of surfaces. *With the exception of the great sphere and the standard tori* (*described under classification headings* (i) *and* (ii) *below*), *it is possible to take* $t = r$ *on an appropriate interval in* $[0, \infty)$ *and obtain the complete surface by taking closures* (*if necessary*) *and extending by rigid reflection. In these cases,* $\theta = \theta(r)$ *satisfies the ordinary differential equation*

$$r\theta'' = 2H_s r\left(\theta'^2 + \frac{1}{r^2+1}\right)^{3/2} - \frac{\theta'}{r^2+1} + (r^2-1)\theta'^3, \tag{3}$$

where H_s *is the mean curvature of the corresponding surface in* $\mathbb{S}^3$. *A first integration of this equation yields*

$$\theta' = \frac{c(r^2+1) - H_s}{\sqrt{(1+r^2)(r^2-(c(r^2+1)-H_s)^2)}}, \tag{4}$$

where c *is a constant of integration. We will use* c *as the second parameter to index the solution surfaces.*

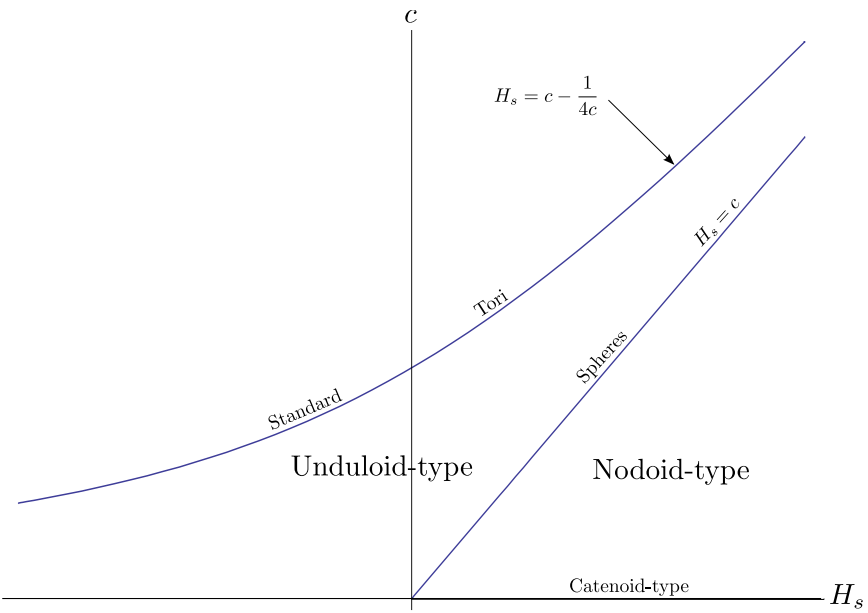

Figure 3. The parameter domain for symmetric CMC surfaces in $\mathbb{S}^3$.

Up to a choice of normal, all surfaces are represented in the parameter region

$$\{(H_s, c) : 0 < c \le (H_s + \sqrt{H_s^2 + 1})/2\} \cup \{(H_s, 0) : H_s \ge 0\}.$$

While the expression (4) is not defined along the curve $c = (H_s + \sqrt{H_s^2 + 1})/2$, *these parameter values correspond naturally to the standard tori*; *see* Figure 3. *All possible complete solution surfaces are as follows.*

Classification.

(i) Spheres ($c = H_s \ge 0$): *For* $H_s \ne 0$, *we find the relation*

$$r = \sqrt{a^2 - (a^2 - 1)\sin^2\theta},$$

where $a = 1/H_s$. *If this expression is used to define* $r = r(\theta)$ *for* θ *in* $0 \le |\theta| \le \theta_{\max} = \sin^{-1}(1/\sqrt{H_s^2 + 1})$, *the expression (2) regularly parameterizes a sphere minus the two points*

$$\{X(\pm\theta_{\max}, \phi)\} = \{(\cos\theta_{\max}, \pm\sin\theta_{\max}, 0, 1)\}$$

on $(-\theta_{\max}, \theta_{\max}) \times \mathbb{R}$.

For $H_s = 0$, *we take* $t = r \in [0, \infty)$ *and* $\theta \equiv 0$; *the expression (2) then parameterizes the open hemisphere* $\{\boldsymbol{x} = (x, y, z, w) \in \mathbb{S}^3 : x > 0, y = 0\}$ *of the (minimal) great sphere* $\{\boldsymbol{x} \in \mathbb{S}^3 : y = 0\}$.

(ii) Standard tori ($c = (H_s + \sqrt{H_s^2+1})/2$): *In this case, we take*

$$r \equiv H_s + \sqrt{H_s^2+1} \tag{5}$$

constant. If $\theta(t) = t$ in (2), we obtain a regular covering map of

$$\{\boldsymbol{x} : x^2 + y^2 = 1/\sqrt{r^2+1},\, z^2 + w^2 = r/\sqrt{r^2+1}\},$$

which is a CMC torus.

(iii) Catenoid-type ($c = 0$, $H_s > 0$): *Integration leads to the relation*

$$\theta = -H_s \int_{H_s}^{r} \frac{1}{\sqrt{(\tau^2+1)(\tau^2-H_s^2)}} d\tau = -\cos\alpha\, F(\cos^{-1}(H_s/r), \alpha),$$

where $\alpha = \sin^{-1}(1/\sqrt{H_s^2+1})$ and F is the standard elliptic integral of the first kind.[1] *Using this formula to define $\theta = \theta(r)$, we can set*

$$\theta_{\max} = -\lim_{r \nearrow +\infty} \theta(r) = \cos\alpha\, K(\alpha)$$

with K the complete elliptic integral of the first kind. Then we can let $r = r(\theta)$ be defined implicitly by the same formula on $(-\theta_{\max}, 0)$. This function has a unique (real analytic) extension to $(-\theta_{\max}, \theta_{\max})$ that is even, convex and unbounded; see Figure 4.

The image of the resulting mapping (2) restricted to $[0, \theta_{\max})$ is an embedded topological cylinder bounded by the circles

$$C_0 = X(\{0\} \times \mathbb{R}) = \left\{\boldsymbol{x} \in \mathbb{S}^3 : y = 0, x = 1/\sqrt{H_s^2+1}\right\}$$

and the great circle

$$C_1 = \lim_{\theta \nearrow \theta_{\max}} X(\{\theta\} \times \mathbb{R}) = \{\boldsymbol{x} \in \mathbb{S}^3 : x = 0 = y\}.$$

The surface extends smoothly (by reflection $y \mapsto -y$) according to the same formula on $-\theta_{\max} < \theta \le 0$. If we extend $r = r(\theta)$ to $(\theta_{\max}, 3\theta_{\max})$ by the formula $r(\theta) = -r(\theta - 2\theta_{\max})$, formula (2) leads to a smooth extension across C_1 by reflection with respect to the plane $x + y\tan\theta_{max} = 0$. More generally, we extend the function $r = r(\theta)$ to be periodic on $\mathbb{R} \setminus \{(2k+1)\theta_{\max} : k \in \mathbb{Z}\}$ with period $4\theta_{\max}$. In this way, the image

$$\mathcal{I}_k = X(((2k-1)\theta_{\max}, (2k+1)\theta_{\max}) \times \mathbb{R})$$

under the map given in (2) is the reflection of $\mathcal{I}_{k+1}$ with respect to the plane $x + y\tan(2k+1)\theta_{\max} = 0$; the union $\mathcal{I}_k \cup \mathcal{I}_{k+1} \cup C_1$ of these two embedded

[1] See Section 2 below for our precise conventions concerning parameters in the elliptic integrals.

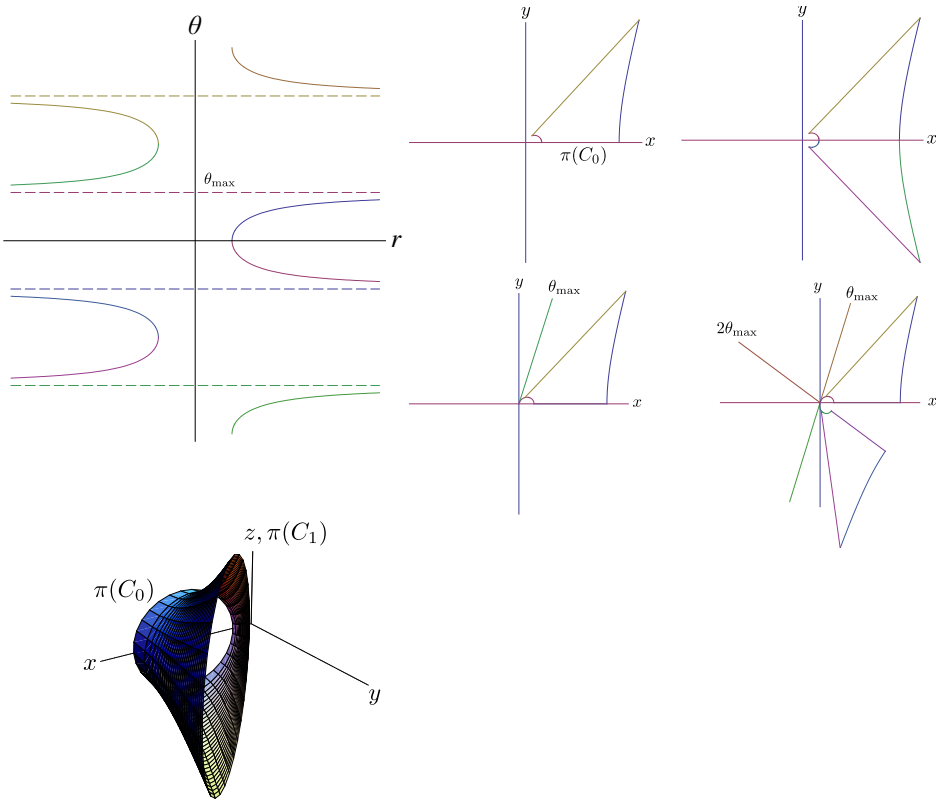

Figure 4. The generating curve for catenoid-type surfaces. Also shown are one "horn" of the stereographic projection of the catenoid-type surface with $H = \pm 1$, and projections that illustrate the extension of the surface from a fundamental domain. The horn is actually only a portion of the (stereographic projection of a) fundamental domain; the fundamental domain occupies the entire sector $0 \le \theta < \theta_{\max}$. The top row projections show first the outline of the projection into the (x, y)-plane of the horn and, second, extension by reflection across C_0. The bottom row shows extension across C_1 (which is the z-axis in the projection).

annuli and the disjoint circle C_1 form a single smooth CMC annulus (*which is embedded if $\theta_{\max} \le \pi/4$*).

The union $\bigcup_k \mathcal{F}_k \cup C_1$ is a strictly immersed topological cylinder. As H_s increases from 0 to ∞, the value of $\theta_{\max}$ increases and takes all values between 0 and $\pi/2$. The immersion is a covering of a torus if and only if $\theta_{\max} = n\pi/(2m)$, where $n, m \in \mathbb{N}$ are relatively prime and $n < m$. In this case, C_1 is covered $2m$ times by the immersion for $0 \le \theta \le 4m\theta_{\max} = 2n\pi$.

(iv) Unduloid-type ($\max\{0, H_s\} < c < (H_s + \sqrt{H_s^2+1})/2$): *For*

$$r_{\min} = \frac{1-\sqrt{1-4c(c-H_s)}}{2c} \le r \le r_{\max} = \frac{1+\sqrt{1-4c(c-H_s)}}{2c},$$

we have the relation

$$\theta = \int_{r_{\min}}^{r} \frac{c\tau^2+c-H_s}{\sqrt{(1+\tau^2)(\tau^2-(c\tau_c^2-H_s)^2)}}\,d\tau = \tag{6}$$

$$\frac{c-H_s}{cr_{\max}d_0} F\left(\sin^{-1}\sqrt{\frac{1-(r_{\min}/r)^2}{1-\mu^2}}, \alpha\right) + \frac{\mu r_{\min}}{d_0}\Pi\left(\nu, \sin^{-1}\sqrt{\frac{1-(r_{\min}/r)^2}{1-\mu^2}}, \alpha\right),$$

where

$$\mu = r_{\min}/r_{\max}, \quad d_0 = \sqrt{1+r_{\min}^2}, \quad \nu = 1-\mu^2, \quad \alpha = \sin^{-1}(\sqrt{\nu}/d_0),$$

and Π *is the standard elliptic integral of the third kind.*[2] *This relation determines an interval*

$$0 \le \theta \le \theta_{\max} = \int_{r_{\min}}^{r_{\max}} \frac{c\tau^2+c-H_s}{\sqrt{(1+\tau^2)[\tau^2-(c\tau_c^2-H_s)^2]}}\,d\tau \tag{7}$$

$$= \frac{c-H_s}{cr_{\max}d_0}K(\alpha) + \frac{\mu r_{\min}}{d_0}\Pi(\nu, \pi/2, \alpha).$$

We may then use (6) to define $r = r(\theta)$ *on* $[0, \theta_{\max}]$ *and extend* r *to be even and periodic with period* $2\theta_{\max}$; *see Figure 5. The resulting immersion (2) has an immersed topological cylinder as image.*

For these unduloid-type surfaces, $\theta_{\max}$ *as a function of* H_s *and* c *is a mapping onto the interval* $(0, \pi)$.

A given unduloid-type immersion is a covering of an immersed torus if and only if $\theta_{\max}$ *is a rational multiple of* π. *Such an immersed torus is embedded if and only if* $\theta_{\max} = \pi/m$ *for some* $m = 1, 2, 3, \ldots$. *This does not occur for* $H_s \le 0$ *or* $m = 1$, *but it does occur for* $H_s > 0$. *In fact, for each* $m = 2, 3, 4, \ldots$ *the relation* $\theta_{\max}(H_s, c_m) = \pi/m$ *defines a unique smooth increasing function* $c_m = c_m(H_s)$ *taking the interval* $[(\cot(\pi/m), (m^2/2-1)/\sqrt{m^2-1}]$ *onto* $[\cot(\pi/m), \sqrt{m^2-1}/2]$. *Each pair of parameters* $(H_s, c_m(H_s))$ *corresponds to an embedded unduloid-type torus with* m *bulges and* m *necks. See Figure 6.*

(v) Nodoid-type ($0 < c < H_s$): *For*

$$r_{\min} = \frac{-1+\sqrt{1-4c(c-H_s)}}{2c} \le r \le r_{\max} = \frac{1+\sqrt{1-4c(c-H_s)}}{2c},$$

[2] See Section 2 below for our precise conventions concerning parameters in the elliptic integrals.

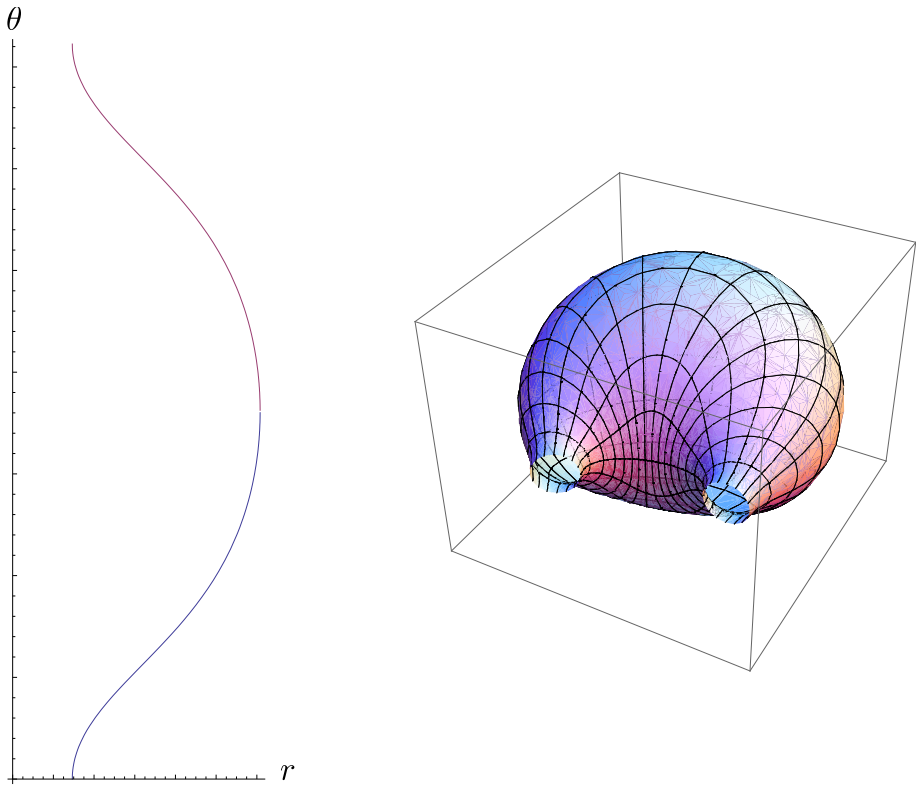

Figure 5. The generating curve for unduloid-type surfaces (one period corresponding to $0 < \theta < 2\theta_{\max}$) and the stereographic projection of two fundamental domains. The parameter values for this surface are $(H_s, c) = (.25, .5)$, and $\theta_{\max} \approx 1.8 > \pi/2$.

we have the relation (6). The function $\theta(r)$ thereby defined is not monotone in this instance, but the inclination angle $\psi = \psi(r)$ satisfying

$$\sin\psi = \frac{\theta'}{\sqrt{1+\theta'^2}}$$

is monotone and allows us to define $r = r(\psi)$ and $\theta = \theta(\psi)$ so that $r(\psi - \pi/2)$ is even and periodic with period 2π, and $\theta(\psi + \pi) = \theta(\psi) + \theta_{\max}$, where $\theta_{\max}$ is given by (7). The resulting generating curve $\gamma : \psi \mapsto (r(\psi), \theta(\psi))$ resembles the meridian of a nodoid; it has nonvanishing curvature and loops toward the θ-axis.

This immersed curve gives rise, via (2), to a strictly immersed cylinder that covers an immersed torus if and only if $\theta_{\max}$ is a rational multiple of π. See Figure 7.

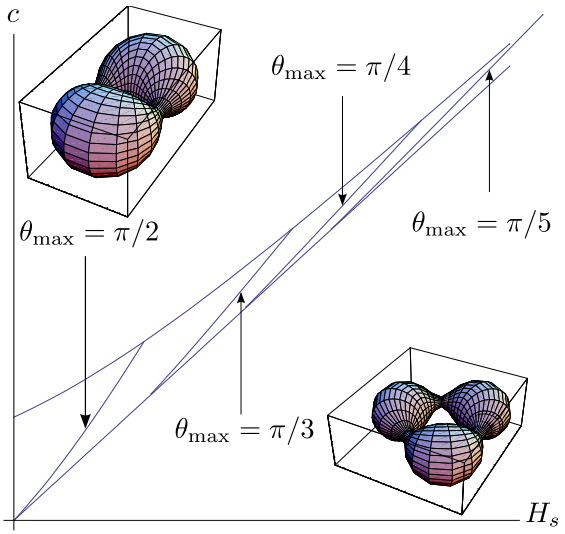

Figure 6. The parameter curves for unduloid-type embedded tori and corresponding examples for $m = 2, 3$.

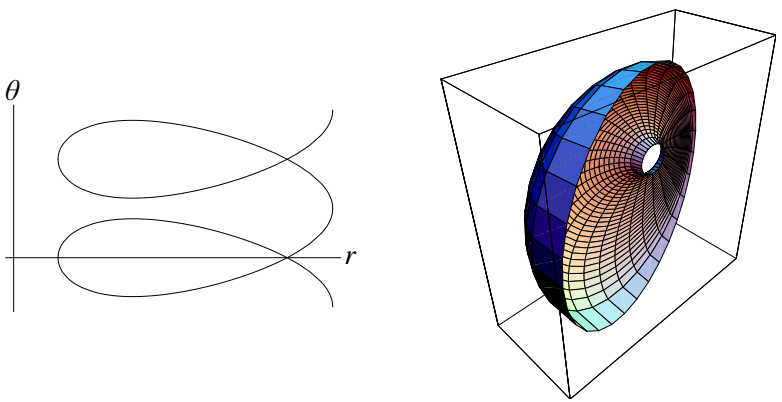

Figure 7. Two periods of the generating curve for a nodoid-type surface and the stereographic projection of one half period of the surface (one fundamental domain).

0.3. ***Radial lines and spherical symmetry.*** One drawback of Definition 1 is that it appears to simply concatenate two unrelated notions of symmetry (having a great circle's worth of great circle reflectional symmetry — which is equivalent to rotational symmetry — or a line's worth of cone point reflectional symmetry). We obtain some unification of these two kinds of symmetry by using radial lines. The

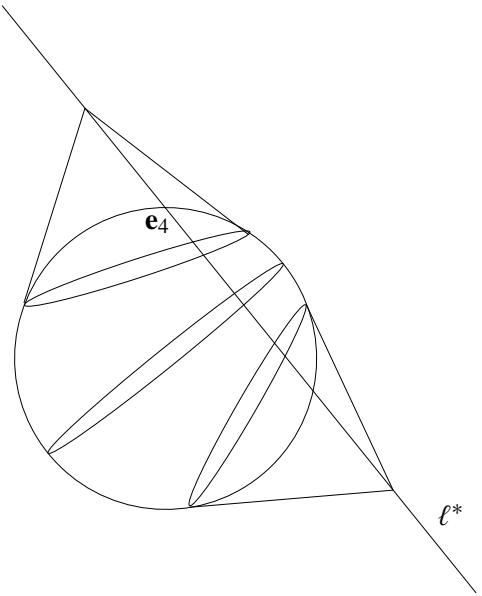

Figure 8. Reflections with the same radial line.

radial line associated to the great circle reflection $g_{\boldsymbol{n}}$ is

$$\ell^* = \{\mathbf{e}_4 + t\boldsymbol{n} : t \in \mathbb{R}\},$$

which passes through the north pole $\mathbf{e}_4 = (0, 0, 0, 1)$ in the direction of $\boldsymbol{n}$. The radial line associated to the cone point reflection $h_{\boldsymbol{y}}$ is

$$\ell^* = \{(1-t)\mathbf{e}_4 + t\boldsymbol{y} : t \in \mathbb{R}\},$$

which passes through $\mathbf{e}_4$ and $\boldsymbol{y}$. If any line $\ell^* = \{\mathbf{e}_4 + t\boldsymbol{v} : t \in \mathbb{R}\}$ through $\mathbf{e}_4$ is specified as a radial line, then a certain family of generalized reflections is specified. The family consists of cone point reflections $h_{\boldsymbol{y}}$ associated to the points in $\ell^* \setminus \overline{B_1(0)}$ and the great circle reflection $g_{\boldsymbol{n}}$, where $\boldsymbol{n} = \boldsymbol{v}/|\boldsymbol{v}|$. The family of generalized reflections associated to ℓ^* is indicated (by symmetry spheres) in Figure 8. The map that associates to a generalized (cone point) reflection a specific point $\boldsymbol{y} \in \ell^*$ is called the radial function. The terminology for radial lines and the radial function will be explained in Section 1 below. We now formulate the definition of spherical symmetry, which takes advantage of this unified viewpoint concerning reflections.

Definition 2 (spherical symmetry). A set $\mathcal{S}$ in $\mathbb{S}^3$ has spherical symmetry if there exists a family Λ of generalized reflections such that

(i) $\mathcal{S}$ is invariant under each map in Λ, and

(ii) There is some line $\Lambda^* = \{\boldsymbol{b} + t\boldsymbol{v} : t \in \mathbb{R}\} \subset \mathbb{R}^4 \setminus \overline{B_1(0)}$ such that

$$\bigcup_{\ell^* \in \mathcal{R}} \ell^* \supset \Lambda^* \cup \{\mathbf{e}_4 + \boldsymbol{v}/|\boldsymbol{v}|\}, \tag{8}$$

where $\mathcal{R}$ is the set of radial lines associated to maps in Λ.

We prove the following classification theorem in Section 3.

Theorem 2. *Any spherically symmetric surface that is compact has special spherical symmetry. Consequently, the compact spherically symmetric CMC surfaces are either*

(i) *spheres*,

(ii) *standard tori*,

(iii) *catenoid-type tori with* $\theta_{\max} = n\pi/(2m)$, *with* $m, n \in \mathbb{N}$ *relatively prime and* $n/m < 1$,

(iv) *unduloid-type tori with* $\theta_{\max} = n\pi/m$, *with* $m, n \in \mathbb{N}$ *relatively prime and* $n/m < 1$, *or*

(v) *nodoid-type tori with* $\theta_{\max} = n\pi/m$.

The embedded examples are spheres, standard tori, and countably many unduloid-type tori corresponding to $\theta_{max} = \pi/m$, *with* $m = 2, 3, 4, \ldots$; *all unduloid-type examples correspond to parameters in our classification with* $H_s > 0$.

Corollary 1. *The only embedded minimal torus with spherical symmetry is the Clifford torus.*

Some authors, for example [Hsiang 1982; Jagy 1998; Park 2002; Brito and Leite 1990], have considered formally the family of rotationally symmetric CMC surfaces generated by an appropriate meridian curve. It turns out that the surfaces described in Theorem 1 are precisely these surfaces, though the parameterization (2) we have chosen does not make this apparent. In the final Section 4 we briefly describe the meridian curves associated to these surfaces.

Still other authors, for example [Ôtsuki 1970; do Carmo and Dajczer 1983], have considered in greater detail the special case of minimal surfaces in this context. Aside from the great sphere, all minimal surfaces are unduloid-type. Thus, our assertion that $\theta_{\max}$ is never π/m for $H_s \leq 0$ generalizes a result of Ôtsuki [1988] asserting that in the minimal case $\pi/2 < \theta_{\max} < \pi/\sqrt{2}$.

1. Preliminaries

Here we discuss the definitions of spherical symmetry introduced above, and we describe in particular the notion of spherical symmetry along a line in $\mathbb{R}^3$. This is an important technical tool in our proofs of the classification theorems.

Recall that stereographic projection

$$\pi : \mathbb{S}^3 \setminus \{\mathbf{e}_4\} \to \mathbb{R}^3, \quad \boldsymbol{x} = (x, y, z, w) \mapsto \frac{1}{1-w}(x, y, z) \tag{9}$$

is a conformal (angle-preserving) diffeomorphism with inverse given by

$$\pi^{-1} : \boldsymbol{x} = (x, y, z) \mapsto \frac{1}{|\boldsymbol{x}|^2+1}(2x, 2y, 2z, |\boldsymbol{x}|^2 - 1).$$

The domain of the mapping π may be extended by the same formula to $\mathbb{R}^4 \setminus \{w = 1\}$. We denote the resulting surjection by $\overline{\pi}$.

Notation. An effort will be made to denote points in $\mathbb{R}^n$ with lowercase boldface letters or by uppercase letters when the image of an immersion is under discussion (see two paragraphs below). The j-th standard basis vector (with 1 in the j-th entry and zeros elsewhere) will be denoted by $\mathbf{e}_j$. The coordinates of points may appear as (x, y, z, w) or (x_1, x_2, x_3, x_4). We will underline points to indicate that they have been projected into a lower dimensional subspace. Thus, when $\boldsymbol{x} = (x, y, z, w)$, the point $\underline{\boldsymbol{x}}$ will denote (x, y, z). Among these conventions, the context should make any ambiguities clear.

By a rotation of $\mathbb{S}^3$, we mean the restriction to $\mathbb{S}^3$ of a linear transformation of $\mathbb{R}^4$ with determinant 1. Similarly, a rotation of $\mathbb{R}^3$ is an element of $\mathrm{SL}_3(\mathbb{R})$. Our discussion could be given with little change in the context of rigid motions, that is, linear transformations with determinant ± 1. Certain special rotations will be important for the discussion below. If R is a rotation of $\mathbb{R}^3$, then the *trivial extension* of R to $\mathbb{R}^4$ is the rotation of $\mathbb{R}^4$ defined by $\mathbf{e}_j \mapsto (R(\underline{\mathbf{e}}_j), 0)$ for $j = 1, 2, 3$ and $\mathbf{e}_4 \mapsto \mathbf{e}_4$. We will denote this trivial extension by the same name R. We denote rotations of the coordinate 2-planes in $\mathbb{R}^4$ by superscripting the rotated coordinates and subscripting the angle. Thus, R_ψ^{xw} is the rotation corresponding to the matrix

$$\begin{pmatrix} \cos\psi & 0 & 0 & -\sin\psi \\ 0 & 1 & 0 & 0 \\ 0 & 0 & 1 & 0 \\ \sin\psi & 0 & 0 & \cos\psi \end{pmatrix}.$$

With this notation, we observe the following result, whose proof may be found in [McCuan and Spietz 1998].

Theorem 3. *Any rotation R of $\mathbb{S}^3 \subset \mathbb{R}^4$ is a composition*

$$R = R_0 \circ R_\psi^{xw} \circ R_\phi^{zw} \circ R_\theta^{xy}, \tag{10}$$

where R_0 is the trivial extension to $\mathbb{R}^4$ of a rotation of $\mathbb{R}^3 = \{(x, y, z, 0)\}$.

Throughout the paper $\mathcal{S}$ will denote the image in $\mathbb{S}^3$ of a smooth immersion $X_0 : M \to \mathbb{S}^3$, where M is a complete, connected two-dimensional Riemannian manifold without boundary. It will be assumed, in general, that the immersion has constant mean curvature and that the image $\mathcal{S} = X_0(M)$ is spherically symmetric. We assume explicitly that M is second countable so that $\mathcal{S}$ has measure zero and has, in particular, dense complement [Hirsch 1994, Proposition 3.1.2].

For $\boldsymbol{n} = (n_1, n_2, n_3, n_4) \in \mathbb{S}^3$ and $0 \le B \le \pi$, the sphere with center $\boldsymbol{n}$ and radius B is $\Gamma = \{\boldsymbol{x} \in \mathbb{S}^3 : \operatorname{dist}(\boldsymbol{x}, \boldsymbol{n}) = B\}$, where the distance is measured intrinsically in $\mathbb{S}^3$. Equivalently, this sphere is given by

$$\Gamma = \{\boldsymbol{x} \in \mathbb{S}^3 : \boldsymbol{x} \cdot \boldsymbol{n} = \cos B\}. \tag{11}$$

The center and radius are not unique but are determined to the extent that they lie among specific pairs $\{(\boldsymbol{n}, B), (-\boldsymbol{n}, \pi - B)\}$. More generally, we recognize (11) as the intersection with $\mathbb{S}^3$ of a hyperplane $\{\boldsymbol{x} \in \mathbb{R}^4 : \boldsymbol{x} \cdot \boldsymbol{y} = |\boldsymbol{y}| \cos B\}$. We say that Γ is nondegenerate if $0 < B < \pi$. In this case, Γ is a smooth submanifold that stereographically projects to a round sphere (or a flat plane if the north pole is in Γ). To be precise, one finds $\pi(\Gamma) = S_\rho(\boldsymbol{a}) \equiv \partial B_\rho(\boldsymbol{a})$, where

$$\boldsymbol{a} = \underline{\boldsymbol{y}}/(|\boldsymbol{y}| \cos B - y_4) \quad \text{and} \quad \rho = |\boldsymbol{y}| \sin B / |y_4 - |\boldsymbol{y}| \cos B|$$

when $\mathbf{e}_4 \notin \Gamma$ and $\pi(\Gamma \setminus \{\mathbf{e}_4\}) = \{\boldsymbol{x} : \boldsymbol{x} \cdot \underline{\boldsymbol{y}} = y_4\}$ otherwise. In this way, stereographic projection provides a one-to-one correspondence between the set of nondegenerate spheres in $\mathbb{S}^3$ and the set of nondegenerate spheres and planes in $\mathbb{R}^3$. For reference, we record the explicit formulas for the inverse stereographic projection of a sphere $S_\rho(\boldsymbol{a})$, which is

$$\{\boldsymbol{x} \in \mathbb{S}^3 : \boldsymbol{x} \cdot (-2\boldsymbol{a}, \rho^2 - |\boldsymbol{a}|^2 + 1) = \rho^2 - |\boldsymbol{a}|^2 - 1\},$$

and a plane $\{\boldsymbol{x} \in \mathbb{R}^3 : \boldsymbol{x} \cdot \boldsymbol{n} = e\}$, which is

$$\{\boldsymbol{x} \in \mathbb{S}^3 : \boldsymbol{x} \cdot (\boldsymbol{n}, e) = e\} \setminus \{\mathbf{e}_4\}.$$

A great sphere in $\mathbb{S}^3$ is one of radius $\pi/2$. Alternatively, a great sphere is the intersection of a hyperplane subspace with $\mathbb{S}^3$. The great spheres are in one-to-one correspondence with the spheres and planes in $\mathbb{R}^3$ passing through a great circle on $\mathbb{S}^2$. A circle in $\mathbb{S}^3$ or $\mathbb{R}^3$ arises as the intersection of two spheres. Aside from degenerate cases, the collection of circles in $\mathbb{S}^3$ is in one-to-one correspondence with the collection of circles and lines in $\mathbb{R}^3$. A great circle is the intersection of two distinct great spheres.

1.1. ***Special spherical symmetry and a parameterization theorem.*** We now consider a surface $\mathcal{S}$ with special spherical symmetry and examine its stereographic

projection $\mathcal{P} = \pi(\mathcal{S} \setminus \{\mathbf{e}_4\})$. We begin by obtaining several refinements of the following basic result.

Lemma 1. *If $\mathcal{S} \subset \mathbb{S}^3$ has special spherical symmetry, then there is a rotation R^s such that $\mathcal{P} = \pi(R^s(\mathcal{S}) \setminus \{\mathbf{e}_4\})$ is rotationally symmetric about an axis in $\mathbb{R}^3$.*

Proof. Let us first assume the symmetry group of $\mathcal{S}$ contains the great sphere reflections $\mathcal{G} = \{g_{\boldsymbol{n}} : \boldsymbol{n} \cdot \boldsymbol{m} = 0 = \boldsymbol{n} \cdot \tilde{\boldsymbol{m}}\}$, where $\boldsymbol{m}$ and $\tilde{\boldsymbol{m}}$ are nonparallel unit vectors. By preliminary rotation, we may assume $\tilde{\boldsymbol{m}} = \mathbf{e}_1$ and $\boldsymbol{m} = (m_1, m_2, 0, 0) \neq \pm\mathbf{e}_1$. In this situation,

$$\mathcal{G} = \{g_{\boldsymbol{n}} : \boldsymbol{n} = (0, 0, n_3, n_4) \in \mathbb{S}^3\}.$$

Our primary interest is in this position, the Apollonian position. Only one of the associated great spheres $G_{\boldsymbol{n}} = \{\boldsymbol{x} \in \mathbb{S}^3 : \boldsymbol{x} \cdot \boldsymbol{n} = 0\}$, namely $G_{\mathbf{e}_3}$, contains $\mathbf{e}_4$. To obtain a specific local parameterization for such a surface, we temporarily consider a rotation to another position in which each of the symmetry spheres contains $\mathbf{e}_4$. Let us, in particular, consider a rotation R^s of $\mathbb{S}^3$ for which $\mathbf{e}_1 \mapsto \mathbf{e}_4$, $\mathbf{e}_2 \mapsto \mathbf{e}_3$, $\mathbf{e}_3 \mapsto -\mathbf{e}_1$, and $\mathbf{e}_4 \mapsto \mathbf{e}_2$. This rotation decomposes as

$$R^s = R^{yz}_{\pi/2} \circ R^{xw}_{\pi/2} \circ R^{zw}_{\pi/2}. \tag{12}$$

The surface $\mathcal{S}_s = R^s(\mathcal{S})$ is now said to be in symmetric position, and $\mathcal{S}_s$ is invariant under the great sphere reflections in $\mathcal{G}_s = \{g_{\boldsymbol{n}} : \boldsymbol{n} = (n_1, n_2, 0, 0) \in \mathbb{S}^3\}$ with corresponding symmetry great spheres $G_{\boldsymbol{n}} = \{\boldsymbol{x} \in \mathbb{S}^3 : \boldsymbol{x} \cdot \boldsymbol{n} = 0\}$, which each contain $\mathbf{e}_4$ and stereographically project to planes

$$P_{\boldsymbol{n}} = \pi(G_{\boldsymbol{n}} \setminus \{\mathbf{e}_4\}) = \{\boldsymbol{x} \in \mathbb{R}^3 : \boldsymbol{x} \cdot \underline{\boldsymbol{n}} = 0\}.$$

Each of these planes contains the z-axis, and a calculation shows that $g_{\boldsymbol{n}} \in \mathcal{G}_s$ induces a standard reflection $\psi_{\boldsymbol{n}}(\boldsymbol{p}) = \boldsymbol{p} - 2(\boldsymbol{p} \cdot \underline{\boldsymbol{n}})\underline{\boldsymbol{n}}$ about $P_{\boldsymbol{n}}$ in $\mathbb{R}^3$. It is well known (see for example [Hopf 1983, Chapter VIII §2]) that this implies $\mathcal{P}_s = \pi(\mathcal{S}_s \setminus \{\mathbf{e}_3\})$ is invariant under all rotations about the z-axis.

We turn next to the situation in which the symmetry group of $\mathcal{S}$ contains the cone point reflections h_y corresponding to the cone points $\boldsymbol{y}$ along a line in $\mathbb{R}^4 \setminus \overline{B_1(0)}$. The conclusion is substantially the same, though the calculation is somewhat more technical, and several of it details generalize the discussion above.

A line in $\mathbb{R}^4 \setminus \overline{B_1(0)}$ may be represented as $\{\boldsymbol{y}_0 + t\boldsymbol{v} : t \in \mathbb{R}\}$, where $\boldsymbol{y}_0$, with $|\boldsymbol{y}_0| > 1$, is the closest point on the line to $\mathbb{S}^3$, $\boldsymbol{v} \in \mathbb{S}^3$, and $\boldsymbol{y}_0 \cdot \boldsymbol{v} = 0$. The horizon sphere $H_{\boldsymbol{y}_0} = \{\boldsymbol{x} \in \mathbb{S}^3 : \boldsymbol{x} \cdot \boldsymbol{y}_0 = 1\}$ intersects the great sphere $G_{\boldsymbol{v}} = \{\boldsymbol{x} \in \mathbb{S}^3 : \boldsymbol{x} \cdot \boldsymbol{v} = 0\}$ in a circle C_0. It is easily checked that

$$C_0 = H_{\boldsymbol{y}_0} \cap G_{\boldsymbol{v}} = H_{\boldsymbol{y}_0 + t\boldsymbol{v}} \cap H_{\boldsymbol{y}_0} = H_{\boldsymbol{y}_0 + t\boldsymbol{v}} \cap G_{\boldsymbol{v}} \quad \text{for all } t \in \mathbb{R} \setminus \{0\},$$

and an explicit parameterization of C_0 is given by

$$\gamma(A) = \frac{\boldsymbol{y}_0}{\alpha^2} + \frac{\sqrt{\alpha^2-1}(\cos A\ \boldsymbol{w}_1 + \sin A\ \boldsymbol{w}_2)}{\alpha} = \frac{1}{\alpha^2}\boldsymbol{y}_0 + \frac{1}{c}(\cos A\ \boldsymbol{w}_1 + \sin A\ \boldsymbol{w}_2),$$

where $\alpha = |\boldsymbol{y}_0|,\ a = 1/\sqrt{\alpha^2-1},\ c = a\alpha = \sqrt{a^2+1}$, and $\{\boldsymbol{w}_1, \boldsymbol{w}_2, \boldsymbol{y}_0/\alpha, \boldsymbol{v}\}$ is an orthonormal basis for $\mathbb{R}^4$.

Using a preliminary rotation, we may assume $\boldsymbol{w}_1 = \mathbf{e}_1,\ \boldsymbol{w}_2 = \mathbf{e}_2,\ \boldsymbol{y}_0 = \alpha\mathbf{e}_3$, and $\boldsymbol{v} = \mathbf{e}_4$. With this normalization, we have

$$\gamma(A) = \cos B\mathbf{e}_3 + \sin B(\cos A\ \mathbf{e}_1 + \sin A\ \mathbf{e}_2),$$

where $\cos B = a/c$ and $\sin B = 1/c$; this is again called the Apollonian position.

We now obtain symmetric position by applying a rotation R^s so that the intersection circle $C_s = R^s(C_0)$ passes through the north pole $\mathbf{e}_4$. One rotation that does this is $R^{yz}_{\pi/2} \circ R^{xw}_B \circ R^{zw}_{\pi/2}$. This choice is fairly straightforward in light of the rotation decomposition theorem (Theorem 3) and the ansatz that the inverse rotation satisfies $\mathbf{e}_4 \mapsto \gamma(0) = \cos B\mathbf{e}_3 + \sin B\mathbf{e}_1$ and, in addition, that $\pi \circ R^s(\cos B\mathbf{e}_3 - \sin B\mathbf{e}_1) = -a\mathbf{e}_1$. More generally, we may apply

$$R^s = R^{yz}_{\pi/2} \circ R^{xw}_B \circ R^{zw}_{\pi/2} \circ R^{xy}_{-A_0},$$

where A_0 is any fixed angle. Note that $R^{xy}_{-A_0}$ leaves C_0 invariant, but moves a specified point $\gamma(A_0)$ to $\gamma(0) = \cos B\mathbf{e}_3 + \sin B\mathbf{e}_1$, so that $R^s \circ \gamma(A_0) = \mathbf{e}_4$.

In symmetric position, therefore, the intersection circle $C_s = R(C_0)$ is parameterized by

$$\begin{aligned}\gamma_s(A) &= \cos B(-\sin B\mathbf{e}_1 + \cos B\mathbf{e}_4)\\ &\quad + \sin B(\cos(A-A_0)(\cos B\mathbf{e}_1 + \sin B\mathbf{e}_4) + \sin(A-A_0)\mathbf{e}_3)\\ &= \cos B \sin B(\cos(A-A_0) - 1)\mathbf{e}_1 + \sin B \sin(A-A_0)\mathbf{e}_3\\ &\quad + (\cos^2 B + \sin^2 B \cos(A-A_0))\mathbf{e}_4.\end{aligned}$$

Note $\gamma_s(A_0) = \mathbf{e}_4$, and the stereographic projection of $C_s \setminus \{\mathbf{e}_4\}$ is parameterized by

$$\begin{aligned}\pi \circ \gamma_s(A) &= -\cot B\mathbf{e}_1 + \csc B\frac{\sin(A-A_0)}{1-\cos(A-A_0)}\mathbf{e}_3\\ &= (-a, c\alpha \sin(A-A_0)/(1-\cos(A-A_0)), 0).\end{aligned}$$

For $A \in (0, 2\pi)$, the function $f(A) = \sin A/(1-\cos A)$ is decreasing and takes all values in $\mathbb{R}$. Thus, $\pi(C_s \setminus \{\mathbf{e}_4\})$ is the vertical line L through $(-a, 0, 0)$ in $\mathbb{R}^3$.

One also checks that $\pi(H_y \setminus \{\mathbf{e}_4\})$, where $\boldsymbol{y} = R^s(\boldsymbol{y}_0 + t\boldsymbol{v}) = -\alpha \sin B\mathbf{e}_1 + t\mathbf{e}_2 + \alpha \cos B\mathbf{e}_4 = -\mathbf{e}_1/a + t\mathbf{e}_2 + \mathbf{e}_4$, is the plane

$$P_y = \{\boldsymbol{x} \in \mathbb{R}^3 : \boldsymbol{x} \cdot (-\mathbf{e}_1/a + t\mathbf{e}_2) = 1\}, \tag{13}$$

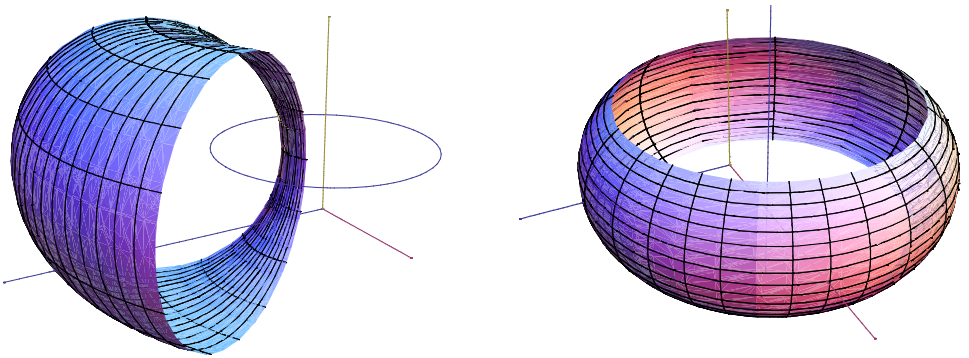

Figure 9. Stereographic projections of an annular surface. At left, Apollonian position; also shown is the image of the circle C_0. At right, symmetric position; notice the horizontal vertical axis $L = \pi(C_s) \setminus \{\mathbf{e}_4\}$ of rotational symmetry.

and $h_{\underline{y}}$ induces the standard reflection $\psi_{\underline{y}}(\boldsymbol{p}) = \boldsymbol{p} - 2(\boldsymbol{p} \cdot \underline{y} - 1)\underline{y}/|\underline{y}|^2$ about $P_{\underline{y}}$ on $\mathbb{R}^3$. All planes containing the vertical line $L = \pi(C_s \setminus \{\mathbf{e}_4\})$ are represented in (13) as t ranges over $\mathbb{R}$, except the x, z-plane. It follows that $\mathcal{P}_s = \pi(R^s(\mathcal{S}) \setminus \{\mathbf{e}_4\})$ is invariant under rotation about the vertical line L. See Figure 9. □

In view of the foregoing discussion, we digress temporarily to prove a parameterization theorem for rotationally symmetric images in $\mathbb{R}^3$.

Theorem 4. *Let $Y : N \to \mathbb{R}^3$ be an immersion of a complete, second countable, two-dimensional manifold N, complete in the metric induced by the immersion and without boundary. Assume the image $Y(N)$ is rotationally symmetric with respect to the vertical axis $L = \{(-a, 0, t) : t \in \mathbb{R}\}$. Then either each connected component N_c of N is diffeomorphic to $\mathbb{R}^2$ and Y is an embedding of each N_c onto a horizontal plane, or there is a point $p_0 \in N$ whose image $\boldsymbol{p}_0 = Y(p_0)$ has the form $(-a + r_0, 0, z_0)$ with $r_0 > 0$, and there is some $\epsilon > 0$, an immersion $\jmath : \mathbb{R} \times (z_0 - \epsilon, z_0 + \epsilon) \to N$ and a smooth positive function $r = r(z)$ defined on $(z_0 - \epsilon, z_0 + \epsilon)$ such that*

(i) $Y \circ \jmath(\theta, z) = (-a + r\cos\theta, r\sin\theta, z)$,

(ii) $\jmath(0, z_0) = p_0$, *and*

(iii) *for every $\theta \in \mathbb{R}$, the restriction $\jmath : (\theta, \theta + 2\pi) \times (z_0 - \epsilon, z_0 + \epsilon) \to N$ is a local parameter chart for N.*

Proof. Evidently, the special case of the theorem when $a = 0$ and L is the z-axis implies the result as stated.

Consider the action R of rotation about the z-axis Z on $\mathbb{R}^3 \setminus Z$. We will use the notations

$$R_\theta(\boldsymbol{x}) = \begin{pmatrix} \cos\theta & -\sin\theta & 0 \\ \sin\theta & \cos\theta & 0 \\ 0 & 0 & 1 \end{pmatrix} \boldsymbol{x} \quad \text{and} \quad \dot{R}_\theta(\boldsymbol{x}) = \begin{pmatrix} -\sin\theta & -\cos\theta & 0 \\ \cos\theta & -\sin\theta & 0 \\ 0 & 0 & 0 \end{pmatrix} \boldsymbol{x}.$$

Note that $\tilde{N} = N \setminus Y^{-1}(L)$ is a nonempty open submanifold of N. Any point $p_0 \in \tilde{N}$ has image $\boldsymbol{p}_0 = Y(p_0) = (r_0 \cos\theta_0, r_0 \sin\theta_0, z_0)$ where $r_0 > 0$. Let $\xi : U \to V \subset \mathbb{R}^2$ be a local coordinate chart on $\tilde{N}$ with $\xi(p_0) = (0,0)$ and such that $Y \circ \xi^{-1}$ is an embedding of V into $\mathbb{R}^3 \setminus L$. Set $\mathcal{S}_0 = Y(U)$.

We claim that $\dot{R}_0(\boldsymbol{p}) \in T_{\boldsymbol{p}}\mathbb{R}^3$ satisfies $\dot{R}_0(\boldsymbol{p}) \in T_{\boldsymbol{p}}\mathcal{S}_0$ for every $\boldsymbol{p} \in \mathcal{S}_0$. In fact, this is obvious from the rotational symmetry, since otherwise $\dot{R}_0(\boldsymbol{p})$ is transverse to $T_{\boldsymbol{p}}\mathcal{S}_0$, and we find $Y(N) \supset \bigcup_\theta R_\theta(\mathcal{S}_0)$, which contains an open set in $\mathbb{R}^3$; this contradicts our assumption that N is second countable since Hirsch shows in [1994, Proposition 3.1.2] that all images of second countable manifolds have empty interior. We thus obtain a nonvanishing vector field

$$\boldsymbol{w}_\xi = (d(Y \circ \xi^{-1})^{-1} \dot{R}_0(Y) \quad \text{on } V \subset \mathbb{R}^2.$$

By reparametrizing V [Chern 1959, Theorem 1.4], we may assume $\boldsymbol{w} = \mathbf{e}_2$, or equivalently $\boldsymbol{w} = \partial/\partial v_2$ in terms of (v_1, v_2)-coordinates on V.

It follows that the images under $Y \circ \xi^{-1}$ of the coordinate lines $v_1 =$ constant in V lie along the circular orbits of R. In fact, $Y \circ \xi^{-1}(v_1, v_2) = R_{v_2}(Y \circ \xi^{-1}(v_1, 0))$ at least locally in some open ball about $(0,0) \in V$, since both expressions satisfy the ODE

$$\frac{d\boldsymbol{x}}{dv_2} = \dot{R}_0(\boldsymbol{x}), \quad \boldsymbol{x}(0) = Y \circ \xi^{-1}(v_1, 0).$$

A local basis for $T_{\boldsymbol{p}}\mathcal{S}_0$, where $\boldsymbol{p} = Y \circ \xi^{-1}(v_1, v_2)$, is thus given by

$$\boldsymbol{u} := \frac{d}{dv_1}(Y \circ \xi^{-1}(v_1, v_2)) \quad \text{and} \quad \dot{R}_0(\boldsymbol{p}).$$

Since these vectors are independent, $\boldsymbol{u} \cdot \mathbf{e}_3 = 0$ if and only if $\underline{Y} = (Y_1, Y_2, 0) \in T_{\boldsymbol{p}}\mathcal{S}_0$.

Let us consider first the possibility that $\underline{Y}(0,0) \in T_{\boldsymbol{p}_0}\mathcal{S}_0$ for every $\boldsymbol{p}_0 \in Y(N) \setminus L$. In this case, we consider

$$\eta : V \to \mathbb{R}^2, \quad (v_1, v_2) \mapsto \chi \circ Y \circ \xi^{-1}(v_1, v_2)$$

where χ is a branch of polar coordinates on $[\theta_0 - \pi, \theta_0 + \pi)$. Note that

$$D\eta(v_1, v_2) = \begin{pmatrix} (Y \cdot \boldsymbol{u})/\chi_1 & 0 \\ (\dot{R}_0(Y) \cdot \boldsymbol{u})/\chi_1^2 & 1 \end{pmatrix}, \quad \text{where } \chi_1 = |\underline{Y}|.$$

In particular, $\det D\eta(0,0) = \boldsymbol{p}_0 \cdot \boldsymbol{u}_0 / r_0$ where $\boldsymbol{u}_0 = \boldsymbol{u}(0,0)$. We are assuming $\boldsymbol{u}_0 \cdot \mathbf{e}_3 = 0$, so $\boldsymbol{u}_0 = (\boldsymbol{u}_0 \cdot \boldsymbol{p}_0)\underline{\boldsymbol{p}}_0 / r_0^2 + (\boldsymbol{u}_0 \cdot \dot{R}_0(\boldsymbol{p}_0))\dot{R}_0(\boldsymbol{p}_0)/r_0^2$. Since $\boldsymbol{u}_0$ and $\dot{R}_0(\boldsymbol{p}_0)$

are linearly independent, we must have $\boldsymbol{u}_0 \cdot \boldsymbol{p}_0 \neq 0$. Thus, η is invertible in some neighborhood $V_0 \subset\subset V$. Setting $U_0 = \xi^{-1}(V_0)$, we have a local coordinate chart $\zeta = \eta \circ \xi : U_0 \to \mathbb{R}^2$ for which $Y \circ \zeta^{-1}(r, \theta) = (r\cos\theta, r\sin\theta, z_0)$. The form of the first two coordinates follows from the definition of η^{-1}; the last coordinate is a consequence of the fact that $\boldsymbol{u} \cdot \mathbf{e}_3 = 0 = \dot{R}_0(Y) \cdot \mathbf{e}_3$.

There exist positive numbers $\epsilon, \delta > 0$ such that

$$(r_0 - \epsilon, r_0 + \epsilon) \times (\theta_0 - \delta, \theta_0 + \delta) \subset \eta(V_0),$$

and we have an immersion

$$\iota = \zeta^{-1} : (r_0 - \epsilon, r_0 + \epsilon) \times (\theta_0 - \delta, \theta_0 + \delta) \to N$$

satisfying $Y \circ \iota(r, \theta) = (r\cos\theta, r\sin\theta, z_0)$ and $\iota(r_0, \theta_0) = p_0$.

We first extend ι to a local diffeomorphism on all of $(0, \infty) \times \mathbb{R}$ onto all of N_c, where N_c is the component of N containing p_0. The resulting map will still satisfy $Y \circ \iota(r, \theta) = (r\cos\theta, r\sin\theta, z_0)$.

Let ι now also denote a maximal extension of $\iota = \zeta^{-1}$ to an open subset Σ of $(0, \infty) \times \mathbb{R}$ such that $Y \circ \iota(r, \theta) = (r\cos\theta, r\sin\theta, z_0)$ and for every $\theta \in \mathbb{R}$, the restriction of ι to $\Sigma \cap (0, \infty) \times (\theta, \theta + 2\pi)$ is a local parameter chart for N. We claim that $\Sigma = (0, \infty) \times \mathbb{R}$. Otherwise, there is some $(r_*, \theta_*) \in \partial\Sigma \cap (0, \infty) \times \mathbb{R}$. Since the point p_0 in the reasoning above was arbitrary in $\tilde{N}$, we may apply the same argument to

$$p_* = \lim_{\Sigma \ni (r,\theta) \to (r_*, \theta_*)} \iota(r, \theta)$$

and obtain a nontrivial extension of ι to a neighborhood of (r_*, θ_*), which contradicts the maximality of ι.

Finally, we set $q_0 = \lim_{r \to 0} \iota(r, \theta)$. Since this point is well defined, we see that $N_c = \iota(\Sigma) \cup \{q_0\}$ is diffeomorphic to $\mathbb{R}^2$.

We now turn to the alternative situation in which there is a point $p_0 \in \tilde{N}$ with

$$Y(p_0) = \boldsymbol{p}_0 = (r_0\cos\theta_0, r_0\sin\theta_0, z_0)$$

and $\underline{Y}(p_0) = (r_0\cos\theta_0, r_0\sin\theta_0, 0) \notin T_{\boldsymbol{p}_0}\mathcal{S}_0$, where $\mathcal{S}_0 = Y(U)$ is the image of a coordinate neighborhood with local coordinate $\xi : U \to V \subset \mathbb{R}^2$ on $\tilde{N}$ with $\xi(p_0) = (0, 0)$ and $Y \circ \xi^{-1}$ an embedding much as above. Continuing the same line of reasoning, we may assume v_1 is the polar displacement in local coordinates v_1, v_2 on V. In this case

$$Y \circ \xi^{-1}(v_1, v_2) = R_{v_1 - \theta_0}(Y \circ \xi^{-1}(0, v_2)) \tag{14}$$

locally near $(0, 0) \in V$ and

$$\boldsymbol{v}(v_1, v_2) := \frac{\partial}{\partial v_2}(Y \circ \xi^{-1}(v_1, v_2))$$

satisfies $\boldsymbol{v} \cdot \mathbf{e}_3 \neq 0$ (also near the origin). We consider the map

$$\begin{aligned}\eta(v_1, v_2) &= (\chi_2 \circ Y \circ \xi^{-1}(v_1, v_2), Y \circ \xi^{-1}(v_1, v_2) \cdot \mathbf{e}_3 \\ &= (\theta_0 + v_1, R_{v_1}(Y \circ \xi^{-1}(0, v_2)) \cdot \mathbf{e}_3) \\ &= (\theta_0 + v_1, Y \circ \xi^{-1}(0, v_2) \cdot \mathbf{e}_3)\end{aligned}$$

and note that

$$D\eta = \begin{pmatrix} 1 & 0 \\ 0 & \boldsymbol{v} \cdot \mathbf{e}_3 \end{pmatrix} \quad \text{where } \boldsymbol{v} = \boldsymbol{v}(0, v_2). \tag{15}$$

In particular, $\det D\eta(0, 0)$ is nonzero, and again we obtain a local coordinate chart $\zeta = \eta \circ \xi : U_0 \to \mathbb{R}^2$ where $V_0 \subset\subset V$ and $U_0 = \xi^{-1}(V_0)$. This time, however, we find

$$Y \circ \zeta^{-1}(\theta, z) = (r \cos\theta, r \sin\theta, z), \quad \text{where } r = r(\theta, z) = \chi_1 \circ Y \circ \zeta^{-1}(\theta, z).$$

We claim that $r = r(z)$ is independent of θ. To see this, we compute

$$\frac{\partial}{\partial\theta}(\chi_1 \circ (Y \circ \xi^{-1}) \circ \eta^{-1}(\theta, z_0)) = \frac{Y \circ \zeta^{-1}(\theta, z)}{\chi_1 \circ Y \circ \zeta^{-1}(\theta, z)} D(Y \circ \xi^{-1}(\eta^{-1}(\theta, z)) \cdot \frac{\partial}{\partial\theta} \cdot (\eta^{-1}(\theta, z)).$$

We have from (15) that

$$D\eta^{-1}(\theta, z) = \frac{1}{\det D\eta(\theta, z)} = \begin{pmatrix} \boldsymbol{v}(\eta^{-1}(\theta, z)) \cdot \mathbf{e}_3 & 0 \\ 0 & 1 \end{pmatrix}.$$

Thus,

$$\frac{\partial}{\partial\theta}(\chi_1 \circ Y \circ \zeta^{-1}(\theta, z)) = \mu Y \circ \zeta^{-1}(\theta, z) \cdot \frac{\partial(Y \circ \xi^{-1})}{\partial v_1}(\eta^{-1}(\theta, z)),$$

where $\mu = \boldsymbol{v}(\eta^{-1}(\theta, z)) \cdot \mathbf{e}_3 / (\chi_1 \circ Y \circ \zeta^{-1}(\theta, z) \det D\eta(\eta^{-1}(\theta, z)))$. On the other hand, using (14),

$$\begin{aligned}\frac{\partial(Y \circ \xi^{-1})}{\partial v_1}(\eta^{-1}(\theta, z)) &= \dot{R}_{\eta_1^{-1}(\theta,z)}(Y \circ \xi^{-1}(0, \eta_2^{-1}(\theta, z))) \\ &= R_{\pi/2 + \eta_1^{-1}(\theta,z)}(Y \circ \xi^{-1}(0, \eta_2^{-1}(\theta, z))) \\ &= R_{\pi/2}(Y \circ \xi^{-1} \circ \eta^{-1}(\theta, z)).\end{aligned}$$

Thus,

$$\frac{\partial}{\partial\theta}(r(\theta, z)) = \mu Y \circ \zeta^{-1}(\theta, z) \cdot R_{\pi/2}(Y \circ \zeta^{-1}(\theta, z)) = 0,$$

and $r = r(\theta)$ as claimed.

We conclude that $\gamma := \zeta^{-1} : (\theta_0 - \delta, \theta_0 + \delta) \times (z_0 - \epsilon, z_0 + \epsilon) \to N$ is a well-defined immersion (for ϵ and δ small enough) that satisfies conditions (i) and (ii)

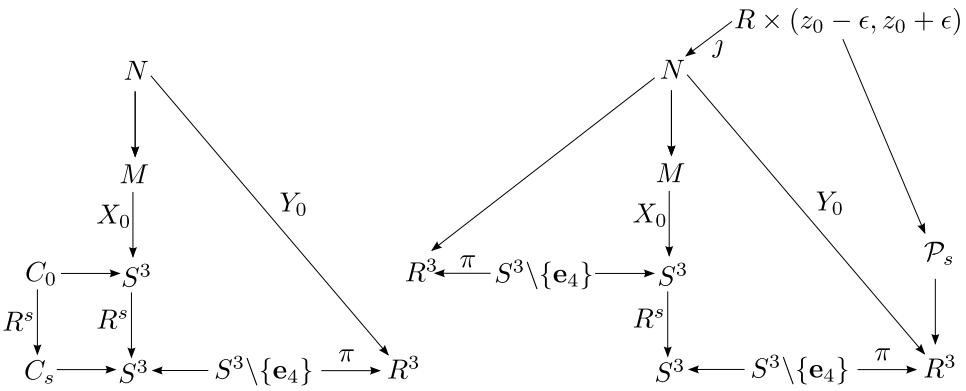

Figure 10. Mappings used to obtain an explicit parameterization. Unlabeled mappings are either identity immersions or compositions as shown.

of the theorem. Finally, we let $\jmath$ also denote an extension to a subset Σ of the strip $\mathbb{R} \times (z_0 - \epsilon, z_0 + \epsilon)$ that is maximal subject to these conditions:

- $\jmath$ is an immersion.
- There is a smooth positive function $r = r(z)$ defined on

$$\Sigma_2 := \{z \text{ such that there exists a } \theta \in \mathbb{R} \text{ with } (\theta, z) \in \Sigma\}$$

  such that $Y \circ \jmath\,(\theta, z) = (r\cos\theta, r\sin\theta, z)$.
- For every $\theta \in \mathbb{R}$, the restriction $\jmath : \Sigma \cap (\theta, \theta + 2\pi) \times (z_0 - \epsilon, z_0 + \epsilon) \to N$ is a local parameter chart for N.

It follows that $\jmath$ satisfies all the conditions of the theorem's second alternative. □

We now return to the CMC immersion $X_0 : M \to \mathbb{S}^3$. In the discussion that follows, the diagrams of Figure 10 display the relations between various submanifolds and maps. We set $N = M \setminus (R^s \circ X_0)^{-1}(\mathbf{e}_4)$ and apply Theorem 4 to $Y_0 = \pi \circ R^s \circ X_0 : N \to \mathbb{R}^3$ to obtain the following basic result.

Lemma 2. *If $X_0 : M \to \mathbb{S}^3$ has image $\mathcal{S}$ with special spherical symmetry, then either $\mathcal{S}$ is a sphere, or (without loss of generality) there is some $\epsilon > 0$ and a nonsingular immersion $\jmath : (-\epsilon, \epsilon) \times \mathbb{R} \to M$, a positive smooth function $r = r(\theta)$ defined on $(-\epsilon, \epsilon)$, a positive constant $\rho_0 > 0$, and another constant h such that $X_0 \circ \jmath$ satisfies*

$$\pi \circ X_0 \circ \jmath\,(\theta, \phi) = (R\cos\theta, R\sin\theta, r\sin\phi + h)$$

where $R = \sqrt{r^2 + \rho_0^2} + r\cos\phi$.

Proof. If Y_0 parameterizes horizontal planes, then we let N_c be any connected component of N. We know $Y_0(N_c) = \{(x, y, h)\}$ for some $h \in \mathbb{R}$, and by the formula for inverse stereographic projection,

$$R^s \circ X_0(N_c) = \{\boldsymbol{x} \in \mathbb{S}^3 : \boldsymbol{x} \cdot (\mathbf{e}_3 + h\mathbf{e}_4) = h\} \setminus \{\mathbf{e}_4\}.$$

Since the image of X_0 is complete, there is some $p_0 \in M$ for which

$$\lim_{p \in N_c, |Y_0(p)| \to \infty} p = p_0 \quad \text{and} \quad R^s \circ X_0(p_0) = \mathbf{e}_4.$$

There is a neighborhood U_0 of p_0 in M such that $U_0 \setminus \{p_0\} \subset N_c$, and it follows that $M = N_c \cup \{p_0\}$ is a sphere with $X_0(M) = R^s\{\boldsymbol{x} \in \mathbb{S}^3 : \boldsymbol{x} \cdot (\mathbf{e}_3 + h\mathbf{e}_4) = h\}$.

If the second alternative of Theorem 4 holds, there is an immersion

$$\jmath : \mathbb{R} \times (z_0 - \epsilon, z_0 + \epsilon) \to N$$

such that $Y_0 \circ \jmath\,(\theta_s, z_s) = (-a + r_s \cos\theta_s, r_s \sin\theta_s, z_s)$ parameterizes an embedded annulus. Since $Y_0 = \pi \circ R^s \circ X_0$, we find

$$\begin{aligned} R^s \circ X_0 \circ \jmath &= \frac{(2(-a + r_s\cos\theta_s), 2r_s\sin\theta_s, 2z_s, a^2 - 2ar_s\cos\theta_s + {r_s}^2 + {z_s}^2 - 1)}{a^2 - 2ar_s\cos\theta_s + {r_s}^2 + {z_s}^2 + 1} \\ &= \frac{(2(-a + r_s\cos\theta_s), 2r_s\sin\theta_s, 2z_s, \mu^2 - 2ar_s\cos\theta_s - 2)}{\mu^2 - 2ar_s\cos\theta_s}, \end{aligned}$$

where $\mu^2 = {r_s}^2 + {z_s}^2 + a^2 + 1$. Note that the s subscripts on r_s, θ_s, and z_s indicate that these are cylindrical coordinates specifically associated with the projection from symmetric position. For z_s fixed, the expression $R^s \circ X_0 \circ \jmath\,(\theta_s, z_s)$ parameterizes a circle $\Gamma_s(z_s)$ in $\mathbb{S}^3$. Since $X_0 \circ \jmath$ is an embedding (mod 2π in θ_s), we know that $\mathbf{e}_4$ can lie in at most one of the Apollonian circles $\Gamma(z_s) := (R^s)^{-1}(\Gamma_s(z_s))$. By adjusting the z_s interval if necessary, we may assume that $\mathbf{e}_4$ does not belong to $\{X_0 \circ \jmath\,(\mathbb{R} \times (z_0 - \epsilon, z_0 + \epsilon)\}$. Thus, $\pi(\Gamma(z_s))$ is a circle in $\mathbb{R}^3$ for every z_s.

Recalling that $c = \sqrt{a^2 + 1} = \csc B$ and $R^s = R^{yz}_{\pi/2} \circ R^{xw}_B \circ R^{zw}_{\pi/2} \circ R^{xy}_{-A_0}$, we find

$$\begin{aligned} R^{xw}_B \circ R^{zw}_{\pi/2} \circ R^{xy}_{-A_0} \circ X_0 \circ \jmath &= \frac{(2(-a + r_s\cos\theta_s), 2z_s, -2r_s\sin\theta_s, \mu^2 - 2ar_s\cos\theta_s - 2)}{\mu^2 - 2ar_s\cos\theta_s}, \\ R^{zw}_{\pi/2} \circ R^{xy}_{-A_0} \circ X_0 \circ \jmath &= \frac{(\mu^2 - 2c^2, 2cz_s, -2cr_s\sin\theta_s, a\mu^2 - 2c^2 r_s\cos\theta_s)}{c(\mu^2 - 2ar_s\cos\theta_s)}, \end{aligned}$$

since $\cos B = a/c$ and $\sin B = 1/c$. Hence,

$$R^{xy}_{-A_0} \circ X_0 \circ \jmath = \frac{(\mu^2 - 2c^2, 2cz_s, a\mu^2 - 2c^2 r_s\cos\theta_s, 2cr_s\sin\theta_s)}{c(\mu^2 - 2ar_s\cos\theta_s)},$$

If $\mu^2-2c^2\equiv 0$ on $(z_0-\epsilon, z_0+\epsilon)$, then $r_s(z_s)\equiv\sqrt{c^2-{z_s}^2}$, and the annular image $\mathcal{P}_s$ of $Y_0\circ\jmath$ is a part of the sphere $\partial B_c(-a,0,0)$. In particular, X_0 is an isometry onto a portion of a great sphere locally near the point p_0.

If μ^2-2c^2 does not vanish identically, we may again adjust the z_s interval and assume

$$\theta=\theta(z_s)=\tan^{-1}\Big(\frac{2cz_s}{\mu^2-2c^2}\Big) \tag{16}$$

is well defined for $z_s\in(z_0-\epsilon, z_0+\epsilon)$. If $\theta'\equiv 0$, then we have an ODE for $r_s=r_s(z_s)$, namely,

$$\Big(\frac{2cz_s}{\mu^2-2c^2}\Big)'\Big/\Big(1+\Big(\frac{2cz_s}{\mu^2-2c^2}\Big)^2\Big)=0,$$

that is, $2z_sr_s{r_s}'-{r_s}^2+{z_s}^2+c^2=0$. The solutions of this equation have the form $r_s(z_s)=\sqrt{c^2-{z_s}^2+2kz_s}$, and $Y_0\circ\jmath$ parameterizes a portion of the sphere $\partial B_{\sqrt{c^2+k^2}}(-a,0,k)$. Again, $X_0\circ\jmath$ parameterizes a portion of a great sphere.

Finally, if θ' does not vanish identically, we may restrict the values of z_s to an interval $(z_0-\epsilon, z_0+\epsilon)$ on which $\theta'(z_s)$ does not vanish. Furthermore, projecting, we have

$$\begin{aligned}\pi\circ R^{xy}_{-A_0}\circ X_0\circ\jmath&=\frac{(\mu^2-2c^2,2cz_s,a\mu^2-2c^2r_s\cos\theta_s)}{c(\mu^2-2ar_s\cos\theta_s-2r_s\sin\theta_s)}\\&=\frac{(\mu^2-2c^2,2cz_s,a\mu^2-2c^2r_s\cos\theta_s)}{c(\mu^2-2cr_s\cos(\theta_s-B))}\\&=\frac{\sqrt{(\mu^2-2c^2)^2+4c^2{z_s}^2}}{c(\mu^2-2cr_s\cos(\theta_s-B))}(\cos\theta,\sin\theta,0)\\&\qquad+\frac{a\mu^2-2c^2r_s\cos\theta_s}{c(\mu^2-2cr_s\cos(\theta_s-B))}(0,0,1).\end{aligned}$$

Notice that if z_s is fixed, then $\theta=\theta(z_s)$ is constant and the last expression is a parameterization of the circle $\pi\circ R^{xy}_{-A_0}(\Gamma(z_s))$ in the plane $y=x\tan\theta$. In order to see this in more convenient coordinates, set

$$\gamma_0(\theta_s,z_s)=\frac{\sqrt{(\mu^2-2c^2)^2+4c^2{z_s}^2}}{c(\mu^2-2cr_s\cos(\theta_s-B))}\quad\text{and}\quad\sigma_0(\theta_s,z_s)=\frac{a\mu^2-2c^2r_s\cos\theta_s}{c(\mu^2-2cr_s\cos(\theta_s-B))}.$$

Again, thinking of z_s as fixed and $\gamma_0=\gamma_0(\theta_s)$, we can take a derivative to find that γ_0 has exactly one maximum ρ_+ at $\theta_s=B$ and one minimum ρ_- at $\theta_s=B+\pi$ on the interval $[0,2\pi)$. The radius of this circle must be $r=(\rho_+-\rho_-)/2$, that is,

$$\begin{aligned}r&=\frac{1}{2c}\Big(\frac{1}{\mu^2-2cr_s}-\frac{1}{\mu^2+2cr_s}\Big)\sqrt{(\mu^2-2c^2)^2+4c^2{z_s}^2}\\&=2r_s\frac{\sqrt{(\mu^2-2c^2)^2+4c^2{z_s}^2}}{\mu^4-4c^2{r_s}^2}=\frac{2r_s}{\sqrt{\mu^4-4c^2{r_s}^2}}.\end{aligned}$$

The last equality uses the fact that $(\mu^2-2c^2)^2+4c^2{z_s}^2=\mu^4-4c^2(\mu^2-c^2-{z_s}^2)$ $=\mu^4-4c^2{r_s}^2$. Similarly, the center of this circle must be $d(\cos\theta_s,\sin\theta_s,0)+h\mathbf{e}_3$, where $h=\sigma_0(B)=\sigma_0(B+\pi)$ and $d=(\rho_+-\rho_-)/2$, that is,

$$h=\cos B \quad \text{and} \quad d=\mu^2\sin B/\sqrt{\mu^4-4c^2{r_s}^2}.$$

Next, we define γ and σ by the equations $\gamma_0=d+r\gamma$ and $\sigma_0=h+r\sigma$. That is,

$$\gamma=\frac{\mu^2\cos(\theta_s-B)-2cr_s}{\mu^2-2cr_s\cos(\theta_s-B)} \quad \text{and} \quad \sigma=\frac{\sin(B-\theta_s)\sqrt{\mu^4-4c^2{r_s}^2}}{\mu^2-2cr_s\cos(\theta_s-B)}.$$

The quantities γ and σ are the cosine and sine of the projected Apollonian angle ϕ appearing in the fundamental parameterization (2), as we will now see. Note first that $\gamma=\gamma(\theta_s)$ has maxima and minima corresponding to those of γ_0 with values 1 and -1 respectively. Thus, the assignment $\cos\phi=\gamma$ is always possible. Also, one can see directly that $\gamma^2+\sigma^2=1$. In fact,

$$\begin{aligned}
&(\mu^2\cos(\theta_s-B)-2cr_s)^2+\sin^2(B-\theta_s)((\mu^2-2c^2)^2+4c^2{z_s}^2)\\
&\quad=\mu^4-4cr_s\mu^2\cos(\theta_s-B)+4c^2({r_s}^2-(\mu^2-c^2-{z_s}^2)\sin^2(\theta_s-B))\\
&\quad=\mu^4-4cr_s\mu^2\cos(\theta_s-B)+4c^2{r_s}^2\cos^2(\theta_s-B)\\
&\quad=(\mu^2-2cr_s\cos(\theta_s-B))^2.
\end{aligned}$$

Thus, the assignments $\cos\phi=\gamma(\theta_s,z_s)$ and $\sin\phi=\sigma(\theta_s,z_s)$, along with the definition of θ given in (16), define ϕ and θ as smooth functions of θ_s and z_s. To see that this defines a nonsingular change of variables, we compute the determinant of $D(\phi,\theta)$. In fact, we already know that $\theta=\theta(z_s)$ and $\theta'\neq 0$. From this we see also that $r=r(\theta)$ is well defined from the definition above. Recalling that $r_s=r_s(z)$, we find

$$D\phi=\frac{(4c^2{r_s}^2-\mu^4,\,2(({2r_s}^2-\mu^2){r_s}'+2r_sz_s)\sin(\theta_s-B))}{\sqrt{\mu^4-4c^2{r_s}^2}(\mu^2-2cr_s\cos(\theta_s-B))}.$$

We need only check that the first coordinate $\partial\phi/\partial\theta_s$ is nonzero. In fact,

$$\mu^4-4c^2{r_s}^2=(\mu^2-2cr_s)(\mu^2+2cr_s)=((r_s-c)^2+{z_s}^2)((r_s+c)^2+{z_s}^2)>0.$$

Thus changing variables, we obtain a local parameterization of $\pi\circ R^{xy}_{-A_0}\circ X_0(M)$ on $(\theta_0-\epsilon_0,\theta_0+\epsilon_0)\times\mathbb{R}$ given by

$$(\theta,\phi)\mapsto(d+r\cos\phi)(\cos\theta,\sin\theta,0)+(h+r\sin\phi)\mathbf{e}_3,$$

where $d=d(\theta)$, $r=r(\theta)$, and $h=\cos B$ is constant. Finally, we set

$$\rho_0=\sqrt{d^2-r^2}=\sqrt{\frac{\mu^4\sin^2B-4{r_s}^2}{\mu^4-4c^2{r_s}^2}}=\sin B$$

and use the arbitrary rotation by A_0 in order to shift the interval for θ to $(-\epsilon_0, \epsilon_0)$; so we obtain a local parameterization $X : (-\epsilon_0, \epsilon_0) \times \mathbb{R} \to \mathbb{R}^3$ of $\mathcal{P}_0 = \pi \circ X_0(M)$ given by

$$X(\theta, \phi) = (\sqrt{\rho_0^2 + r^2} + r\cos\phi)(\cos\theta, \sin\theta, 0) + (h + r\sin\phi)\mathbf{e}_3.$$

We conclude that, aside from the case of spheres, all CMC surfaces with special spherical symmetry have stereographic projections that can be parameterized in this way. For our classification, this is the basic expression with which we will work. The one unknown function is $r = r(\theta)$, and we need to derive (and solve) the ordinary differential equation corresponding to constant mean curvature in $\mathbb{S}^3$. It will be convenient to write this expression as

$$X(\theta, \phi) = R\boldsymbol{u}_1 + (h + r\sin\phi)\mathbf{e}_3, \tag{17}$$

with $R = d + r\cos\phi$ and $d^2 = r^2 + \rho_0^2$.

Before turning to this classification, we briefly describe spherical symmetry in terms of stereographic projection and point out the key differences making it a (much) more general notion.

1.2. ***Interpreting spherical symmetry.*** Given a line $\Lambda^* = \{\boldsymbol{b} + t\boldsymbol{v} : t \in \mathbb{R}\}$, we may often assume $\boldsymbol{b} \perp \boldsymbol{v}$, and this assumption will be made below whenever possible and convenient.

If $\mathcal{S} \subset \mathbb{S}^3$ has special spherical symmetry and is invariant with respect to cone point reflections

$$h_{\boldsymbol{y}}(\boldsymbol{x}) = \boldsymbol{y} + (|\boldsymbol{y}|^2 - 1)\frac{\boldsymbol{x} - \boldsymbol{y}}{|\boldsymbol{x} - \boldsymbol{y}|^2}$$

for $\boldsymbol{y} \in \Lambda^* = \{\boldsymbol{b} + t\boldsymbol{v} : t \in \mathbb{R}\}$, some line in $\mathbb{R}^4 \setminus \overline{B_1(0)}$, then a straightforward calculation shows that for $\boldsymbol{x}$ fixed

$$\lim_{t\to\infty} h_{\boldsymbol{b}+t\boldsymbol{v}}(\boldsymbol{x}) = \boldsymbol{x} - 2(\boldsymbol{x}\cdot\boldsymbol{n})\boldsymbol{n} = g_{\boldsymbol{n}}(\boldsymbol{x}),$$

where $\boldsymbol{n} = \boldsymbol{v}/|\boldsymbol{v}|$ and $g_{\boldsymbol{n}}$ is a great sphere reflection. Thus, for bounded sets like $\mathcal{S}$, we have $g_{\boldsymbol{n}}(\mathcal{S}) = \lim_{t\to\infty} h_{\boldsymbol{b}+t\boldsymbol{v}}(\mathcal{S}) = \mathcal{S}$. Hence, the set Λ of all generalized reflections under which $\mathcal{S}$ is invariant contains $\{h_{\boldsymbol{b}+t\boldsymbol{v}} : t \in \mathbb{R}\} \cup \{g_{\boldsymbol{v}/|\boldsymbol{v}|}\}$. The radial line associated with $h_{\boldsymbol{b}+t\boldsymbol{v}}$ is

$$\ell^* = \{(1-\tau)\mathbf{e}_4 + \tau(\boldsymbol{b} + t\boldsymbol{v}) : \tau \in \mathbb{R}\} \ni \boldsymbol{b} + t\boldsymbol{v},$$

and the radial line associated with $g_{\boldsymbol{v}/|\boldsymbol{v}|}$ is

$$\ell^* = \{\mathbf{e}_4 + \tau\boldsymbol{v}/|\boldsymbol{v}| : \tau \in \mathbb{R}\} \ni \mathbf{e}_4 + \boldsymbol{v}/|\boldsymbol{v}|.$$

We have thus shown half of the following result.

Lemma 3. *If $\mathcal{S} \subset \mathbb{S}^3$ has special spherical symmetry, $\mathcal{S}$ has spherical symmetry.*

To see the other half of the proof, we must consider the case in which $\mathcal{S}$ is invariant with respect to $\Lambda = \{g_{\boldsymbol{n}} : \boldsymbol{n}\cdot\boldsymbol{m} = 0 = \boldsymbol{n}\cdot\tilde{\boldsymbol{m}}\}$, where $\boldsymbol{m}$ and $\tilde{\boldsymbol{m}}$ are nonparallel unit vectors. In this case, we first observe that

$$\bigcup_{\ell^* \in \mathcal{R}} \ell^* = \{\mathbf{e}_4 + \tau\boldsymbol{n} : \tau \in \mathbb{R},\ \boldsymbol{n}\cdot\boldsymbol{m} = 0 = \boldsymbol{n}\cdot\tilde{\boldsymbol{m}}\}.$$

Fixing any $g_{\boldsymbol{n}_0} \in \Lambda$, we can construct an orthonormal basis $\{\boldsymbol{m}, \tilde{\boldsymbol{m}}, \boldsymbol{n}_0, \boldsymbol{v}\}$ for $\mathbb{R}^4$. Setting $\boldsymbol{b} = \mathbf{e}_4 + 3\boldsymbol{n}_0$, we claim that

$$\Lambda^* = \{\boldsymbol{b} + t\boldsymbol{v} : t \in \mathbb{R}\}$$

satisfies requirement (ii) of Definition 2. First note that $|\boldsymbol{b}+t\boldsymbol{v}| \geq |3\boldsymbol{n}_0+t\boldsymbol{v}|-|\mathbf{e}_4| \geq 3-1=2$. Thus, $\Lambda^* \subset \mathbb{R}^4 \setminus \overline{B_1(0)}$. Second, $3\boldsymbol{n}_0+t\boldsymbol{v}$ is orthogonal to both $\boldsymbol{m}$ and $\tilde{\boldsymbol{m}}$. Thus, $3\boldsymbol{n}_0 + t\boldsymbol{v} = \tau\boldsymbol{n}$, where $\tau = |3\boldsymbol{n}_0 + t\boldsymbol{v}| \in \mathbb{R}$ and $\boldsymbol{n} = (3\boldsymbol{n}_0 + t\boldsymbol{v})/|3\boldsymbol{n}_0 + t\boldsymbol{v}|$ is orthogonal to both $\boldsymbol{m}$ and $\tilde{\boldsymbol{m}}$. It follows that $\boldsymbol{b} + t\boldsymbol{v} = \mathbf{e}_4 + 3\boldsymbol{n}_0 + t\boldsymbol{v} = \mathbf{e}_4 + \tau\boldsymbol{n}$, which belongs to $\bigcup_{\ell^* \in \mathcal{R}} \ell^*$. Finally, $\mathbf{e}_4 + \boldsymbol{v}/|\boldsymbol{v}| = \mathbf{e}_4 + \boldsymbol{v}$ and $\boldsymbol{v}\cdot\boldsymbol{m} = 0 = \boldsymbol{v}\cdot\tilde{\boldsymbol{m}}$. Thus, $\mathcal{S}$ has spherical symmetry. □

Having shown that special spherical symmetry is a special case of spherical symmetry, we turn our attention to a set $\mathcal{S} \subset \mathbb{S}^3$ with spherical symmetry and make some basic observations concerning the stereographic projection $\mathcal{P} = \pi(\mathcal{S} \setminus \{\mathbf{e}_4\})$.

As usual, we assume $\Lambda^* = \{\boldsymbol{b} + t\boldsymbol{v} : t \in \mathbb{R}\}$ in Definition 2 is given with $\boldsymbol{b} \perp \boldsymbol{v}$. After a preliminary rotation of $\mathbb{R}^4$, we may also assume

$$\Lambda^* = \{-a\mathbf{e}_1 + t\mathbf{e}_3 : t \in \mathbb{R}\} \subset \mathbb{R}^3 \subset \mathbb{R}^4.$$

Let $\boldsymbol{p} \in \Lambda^*$ and $f \in \Lambda$ with radial line ℓ^* passing through $\boldsymbol{p}$. It is easy to check that the projection of the symmetry sphere S of f (where $S = G_{\boldsymbol{n}}$ or $S = H_{\boldsymbol{y}}$ as in Section 0.1) passes through $\mathbf{e}_4$ only if the radial line ℓ^* of f lies in the $x_4 = 1$ hyperplane. Since Λ^* does not intersect this plane, the projection of S is a sphere $\partial B_\rho(\boldsymbol{a})$ in $\mathbb{R}^3$. It follows that $\mathcal{P} \setminus \{\boldsymbol{a}\}$ is invariant under the transformation given in (18). One can check, furthermore, that $\pi(\ell^*) = \{\boldsymbol{a}\} = \underline{\boldsymbol{p}}$. In particular, the centers of the projected spheres comprise the points along a line L in $\mathbb{R}^3$.

Note that spherical symmetry does not specify the radius ρ of $\partial B_\rho(\boldsymbol{a})$ as does special spherical symmetry since, in that case, taking $\boldsymbol{b} = -a\mathbf{e}_1$ and $\boldsymbol{a} = -a\mathbf{e}_1 + t\mathbf{e}_3$, we have $\rho = \rho(t) = \sqrt{\rho_0^2 + (h-t)^2}$, where ρ_0 and h are given constants. This is the key difference. In this regard, it is useful to note that the cone points $\boldsymbol{y}$ in a radial line (any line passing through the north pole but not lying in $x_4 = 1$) correspond to spheres in $\mathbb{S}^3$ that project to concentric spheres in $\mathbb{R}^3$. Hence, specifying the radial line ℓ^* of a reflection specifies the center of a sphere in $\mathbb{R}^3$; specifying the specific cone point $\boldsymbol{y}$ on ℓ^* specifies both the center and radius of $\partial B_\rho(\boldsymbol{a}) = \pi(H_{\boldsymbol{y}})$. With this in mind, we formulate the following property of $\mathcal{P}$.

Definition 3 (spherical symmetry along a line in $\mathbb{R}^3$). A set $\mathcal{P} \subset \mathbb{R}^3$ has spherical symmetry along a line if there is some line L in $\mathbb{R}^3$ and for each $\boldsymbol{a} \in L$, there is some radius $\rho > 0$ such that $\mathcal{P} \setminus \{\boldsymbol{a}\}$ is invariant under the map

$$\boldsymbol{p} \mapsto \rho^2 \frac{\boldsymbol{p}-\boldsymbol{a}}{|\boldsymbol{p}-\boldsymbol{a}|^2} + \boldsymbol{a}. \tag{18}$$

The following result is immediate from the discussion above.

Lemma 4. *If $\mathcal{S} \subset \mathbb{S}^3$ has spherical symmetry, there is some rotation R of $\mathbb{S}^3$ such that $\mathcal{P} = \pi(R(\mathcal{S}) \setminus \{\mathbf{e}_4\})$ has spherical symmetry along a line. Conversely, if $\mathcal{P} \subset \mathbb{R}^3$ has spherical symmetry along a line L, and $\mathcal{P} \cap L = \phi$, then $\mathcal{S} = \pi^{-1}(\mathcal{P}) \subset \mathbb{S}^3$ has spherical symmetry.*

It is not known, in general, if surfaces with spherical symmetry admit convenient parameterization. We sharpen the observations of this section in Section 3 and show that compact surfaces with spherical symmetry are well behaved.

2. CMC surfaces with special spherical symmetry

Consider a local projected immersion $\mathcal{P}$ with parameterization of the form (17):

$$X(\theta, \phi) = R\boldsymbol{u}_1 + (h + r\sin\phi)\mathbf{e}_3 \tag{19}$$

on $(-\epsilon, \epsilon) \times \mathbb{R}$ with $r = r(\theta)$ some smooth function and $R = \sqrt{r^2 + \rho_0^2} + r\cos\phi$; $\rho_0 \in (0, 1)$ and h are constants. We also have an initial condition $r(0) = r_0 > 0$. It will be convenient to let $d = d(\theta) = \sqrt{r^2 + \rho_0^2}$ as above. Calculating the mean curvature H_s of $\mathcal{S}$ at $X_0 = \pi^{-1} \circ X$ we find [Park 2002]

$$H_s = \tfrac{1}{2}(1 + |X|^2)H + X \cdot N$$

where H is the Euclidean mean curvature of $\mathcal{P}$ and N is the normal to $\mathcal{P}$ at $X = X(\theta, \phi)$. Here the s subscript indicates the mean curvature with respect to $\mathbb{S}^3$. It is easily checked that

$$\frac{\partial H}{\partial \phi}\bigg|_{\phi=0} = 0.$$

Thus, we find

$$0 = \frac{\partial H_s}{\partial \phi}\bigg|_{\phi=0} = (HX \cdot X_\phi + X \cdot N_\phi)|_{\phi=0}. \tag{20}$$

We recall the expression for $\boldsymbol{u}_1$ and introduce notation for its derivative:

$$\boldsymbol{u}_1 = (\cos\theta, \sin\theta, 0) \quad \text{and} \quad \boldsymbol{u}_2 = (-\sin\theta, \cos\theta, 0).$$

Of course, $\boldsymbol{u}_1$, $\boldsymbol{u}_2$, and $\mathbf{e}_3$ form an orthonormal basis.

A somewhat lengthy calculation, outlined below, provides these formulas:

$$
\begin{aligned}
X_\phi|_{\phi=0} &= (-r\sin\phi \boldsymbol{u}_1 + r\cos\phi \mathbf{e}_3)|_{\phi=0} = r\mathbf{e}_3,\\
N|_{\phi=0} &= \frac{1}{\sqrt{r'^2+d^2}}(d\boldsymbol{u}_1 - r'\boldsymbol{u}_2),\\
N_\phi|_{\phi=0} &= \frac{d}{\sqrt{r'^2+d^2}}\mathbf{e}_3,\\
H|_{\phi=0} &= \frac{a_0+a_1+a_2}{2r(r+d)^2(r'^2+d^2)^{3/2}}
\end{aligned}
\tag{21}
$$

where

$$
\begin{aligned}
a_0 &= d(rd^2r'' - (r^2+d^2)r'^2 - d^4),\\
a_1 &= r(rd^2r'' - (4r^2+3\rho_0^3)r'^2 - 3d^4),\\
a_2 &= -2r^2d(r'^2+d^2).
\end{aligned}
$$

Substituting the first three formulas into (20), we find

$$0 = h(rH|_{\phi=0} + d/\sqrt{r'^2+d^2}).$$

If $h \neq 0$, then $H|_{\phi=0} = -d/(r\sqrt{r'^2+d^2})$. Comparing this equation with (21), we arrive at

$$(r^2+\rho_0^2)rr'' + \rho_0^2 r'^2 + (r^2+\rho_0^2)^2 = 0. \tag{22}$$

Given $r_0 = r(0) > 0$ and $v_0 = r'(0)$, there are unique values of $a > 0$ and $\theta_1 \in (-\pi, \pi)$ for which the solution is given by

$$r = \sqrt{(a^2+\rho_0^2)\cos^2(\theta-\theta_1) - \rho_0^2}, \tag{23}$$

which correspond to a (portion of a) sphere. It can be checked that

$$a^2 = r_0^2(1 + v_0^2/(r_0^2+\rho_0^2))$$

and θ_1 is determined by

$$\cos\theta_1 = \frac{r_0^2+\rho_0^2}{\sqrt{(r_0^2+\rho_0^2)^2 + r_0^2v_0^2}} \quad \text{and} \quad \sin\theta_1 = \frac{r_0v_0}{\sqrt{(r_0^2+\rho_0^2)^2 + r_0^2v_0^2}}.$$

Of course, formal solutions can be obtained with θ_1 in other intervals; this does not affect the values of $r = r(\theta)$, but such an interval will not contain the normalized initial value $\theta_0 = 0$. It is instructive to write the ODE (22) as the equivalent system

$$
\begin{cases}
r' = v\\
v' = -(\rho_0^2v^2 + (r^2+\rho_0^2)^2) \;/\; (r(r^2+\rho_0^2))
\end{cases}
$$

whose phase diagram is shown in Figure 11 along with the geometrical quantities associated with the corresponding spherical solutions.

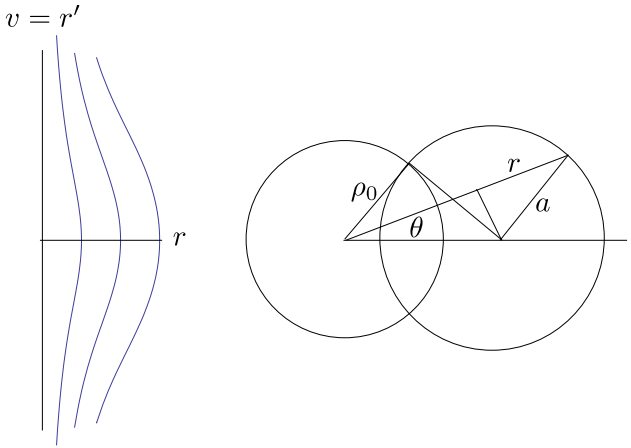

Figure 11. Spherical solutions with nonstandard projection.

From these considerations, we the following lemma is immediate.

Lemma 5. *Unless $\mathcal{S}$ is a sphere, we must have $h = 0$.*

Corollary 2. *Unless $\mathcal{S}$ is a sphere, we must also have $\rho_0 = 1$.*

Proof. This is immediate once we recall that $h = \cos B$ and $\rho_0 = \sin B$ with $B \in (0, \pi/2]$ determined by the original surface. Since $h = 0$, we must have $B = \pi/2$ and $\rho_0 = 1$. The surface must therefore fall back into the class of surfaces that may be stereographically projected (at least locally) to rotationally symmetric ones in $\mathbb{R}^3$. □

We outline below the long calculation alluded to above for the parameterization

$$X(\theta, \phi) = R\boldsymbol{u}_1 + r \sin\phi \mathbf{e}_3. \tag{24}$$

The first and second order quantities mentioned above do not depend on h; we will include the constant $\rho_0 \in (0, 1]$, though in the end, we will use Corollary 2 and specialize to the case $\rho_0 = 1$.

$$N = \frac{X_\theta \times X_\phi}{|X_\theta \times X_\phi|} = \frac{d\cos\phi\,\boldsymbol{u}_1 - r'\boldsymbol{u}_2 + d\sin\phi\,\mathbf{e}_3}{\sqrt{r'^2 + d^2}},$$

$$E = |X_\theta|^2 = r^2\cos^2\phi + 2r(d + 1/d)\cos\phi + (1 + r^2/d^2)r'^2 + d^2,$$

$$F = X_\theta \cdot X_\phi = -(r^2 r'/d)\sin\phi,$$

$$G = |X_\phi|^2 = r^2,$$

$$e = X_{\theta\theta} \cdot N = \frac{-rd\cos^2\phi + (rr'' - r^2 r'^2/d^2 - r'^2 - d^2)\cos\phi - 2rr'^2/d + dr''}{\sqrt{r'^2 + d^2}},$$

$$f = X_{\theta\phi} \cdot N = (rr'/\sqrt{r'^2 + d^2})\sin\phi,$$

$$
\begin{aligned}
g &= X_{\phi\phi}\cdot N = -rd/\sqrt{r'^2+d^2},\\
X\cdot N &= (d/\sqrt{r'^2+d^2})(d\cos\phi + r),\\
H &= \frac{eG-2fF+gE}{2(EG-F^2)} = \frac{a_0+a_1\cos\phi+a_2\cos^2\phi}{2rR^2(r'^2+d^2)^{3/2}},\\
a_0 &= d(rd^2r'' - (r^2+d^2)r'^2 - d^4),\\
a_1 &= r(rd^2r'' - (r^2+3d^2)r'^2 - 3d^4),\\
a_2 &= -2r^2d(r'^2+d^2),\\
H_s &= \tfrac{1}{2}(1+|X|^2)H + X\cdot N = \frac{c_0+c_1\cos\phi+c_2\cos^2\phi}{4rR^2(r'^2+d^2)^{3/2}},\\
c_0 &= d(rd^2(r^2+d^2+1)r'' - (r^2+d^2+(r^2-d^2)^2)r'^2 + d^4(3r^2-d^2-1)),\\
c_1 &= r(rd^2(r^2+3d^2+1)r'' - (r^2+3d^2+(r^2-d^2)^2)r'^2 + d^4(5r^2-d^2-3)),\\
c_2 &= 2r^2d(rd^2r'' - r'^2 + (r^2-1)d^2).
\end{aligned}
$$

Finally, we obtain for $\rho_0 = 1$

$$
H_s = \frac{\sqrt{r^2+1}(r(r^2+1)r'' - r'^2 + r^4 - 1)}{2r(r'^2+r^2+1)^{3/2}}. \tag{25}
$$

It is important to note that (25) depends on the particular parameterization we have chosen, but not essentially. To be more precise, the mean curvature of a given surface depends on a choice of normal, and the opposite choice of normal results in a change in sign of the mean curvature. The expression we have obtained is for a particular choice of normal ("outward" for the local annular patch in the stereographic projection). Because we are considering all possible signs of the mean curvature, we will obtain all possible portions of surfaces with local parameterization of this form. It is possible, however (and it does happen) that two annular portions of a surface can fit together along a circle (singular with respect to (24)) to form a single smooth piece of constant mean curvature surface; one piece will have mean curvature H_s given by (25), and the other will have mean curvature $-H_s$ according to the same formula. Such surfaces all fall into the nodoid-type class, and this technicality will be discussed further below when it becomes an issue.

We are now in a position to prove Theorem 1. We begin by considering the system corresponding to (25) in the $r > 0$ halfplane:

$$
\begin{cases}
r' = v,\\
v' = 2H_s\left(1+\dfrac{v^2}{r^2+1}\right)^{3/2} + \dfrac{1}{r}\left(1+\dfrac{v^2}{r^2+1}\right) - r.
\end{cases} \tag{26}
$$

A unique equilibrium point occurs for the system (26) at $(r, v) = (r_*, 0)$, where r_* is a solution of the equation $r^2 - 2H_s r - 1 = 0$, which is easily solved to obtain (5). The Clifford torus lies in a collection of anchor ring solutions that project to

$$\left\{(\sqrt{r_*^2+1} + r_* \cos\phi)(\cos\theta, \sin\theta, 0) + r_* \sin\phi \mathbf{e}_3 : \theta, \phi \in \mathbb{R}\right\}.$$

These anchor rings become, as H_s tends to $-\infty$ due to our choice of normal, thin tubes around the great circle $\{x^2 + y^2 = 1\}$.

More generally, in any solution with initial condition $(r_0, 0)$ and $r_0 \neq r_*$, the point(s) with $v = 0$ is isolated. (If $0 < r_0 < r_*$, then $v'(\theta_0) = -(r_0^2 - 2H_s r_0 - 1) > 0$; if $r_* < r_0$, then $v'(\theta_0) < 0$.) Consequently, aside from the standard tori (anchor ring solutions), all solutions may be pieced together along circles from annular pieces that may be parameterized as

$$X(r, \phi) = (\sqrt{r^2+1} + r\cos\phi)(\cos\theta, \sin\theta, 0) + r\sin\phi\, \mathbf{e}_3, \tag{27}$$

where $\theta = \theta(r)$. This is the only fact we will use for now about the system (26), whose phase diagrams for representative values of H_s, namely, 0 and ± 1, are shown in Figure 12. We will note for future reference one important observation.

Lemma 6. *If (r, v) is a solution of (26), then $(\tilde{r}(\theta), \tilde{v}(\theta)) = (r(-\theta), -v(-\theta))$ is also a solution. Consequently, the phase diagram for (26) is symmetric with respect to the r axis; solutions satisfying $r'(0) = 0$ are even.*

We note concerning the phase diagrams that each nodoid trajectory (the ones asymptotic to vertical lines) having $H_s < 0$ fits together with a nodoid trajectory having $H_s > 0$ and asymptotic to the same line. One may also match the solutions indicated in the phase diagrams with those represented on two vertical lines in the parameter domain indicated in Figure 13; move downward for $H_s < 0$ and upward for $H_s > 0$. The phase diagrams of Figure 12 are numerically generated, and the precise global properties of all trajectories will not be evident until we finish the proof of Theorem 1; then they may be determined from the explicit formulas.

Before working directly with the equation for $\theta = \theta(r)$, we briefly return to Equation (25). Whenever $v = r' \neq 0$, there is a locally defined smooth function $u = u(r)$ such that $u(r) = r'$. Consequently, $r'' = u'r' = uu'$ and (25) may be rewritten as

$$\frac{ru}{(u^2+r^2+1)^{3/2}} = \frac{u^2 - r^4 + 1}{(r^2+1)(u^2+r^2+1)^{3/2}} + \frac{2H_s r}{(r^s+1)^{3/2}}.$$

Thinking of this equation as $M(r, u)u' = N(r, u)$ and making a standard search for an integrating factor $\phi = \phi(r)$, we find that $\phi = 1/\sqrt{r^2+1}$ and

$$\left(\frac{r}{\sqrt{(u^2+r^2+1)(r^2+1)}} + \frac{H_s}{r^2+1}\right)' = 0.$$

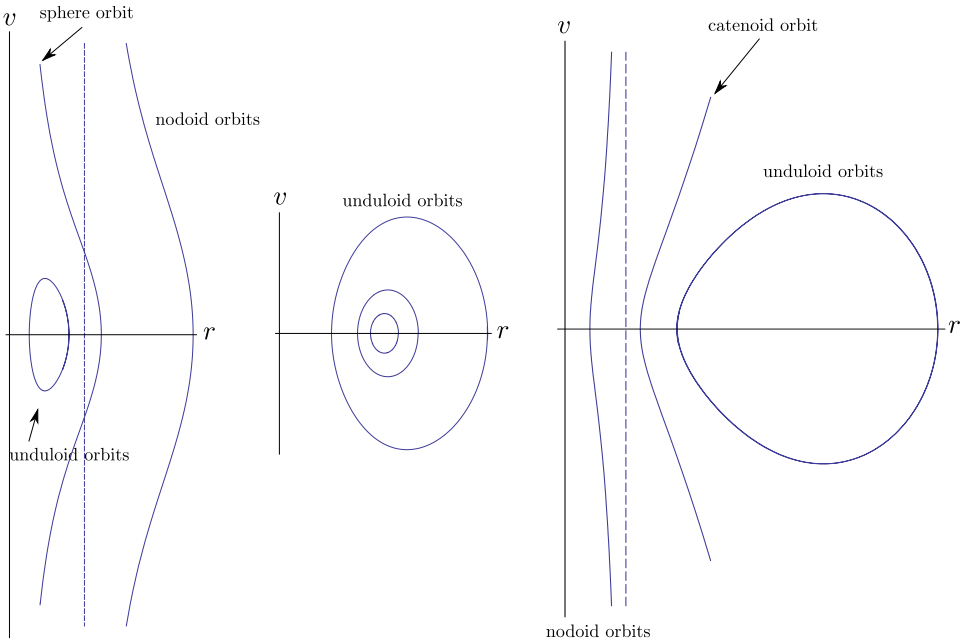

Figure 12. Phase portraits of solutions $r = r(\theta)$ for $H_s < 0$ (left), $H_s = 0$ (center) and $H_s > 0$ (right). The nodoid-type solutions shown (with asymptotes) correspond to only a portion of a fundamental domain. In this particular figure we also see the correspondence of nodoid-type solutions because the figure on the left is for $H_s = -1$, the one on the right is for $H_s = 1$, and the nodoid-type solutions indicated ($c = 3/5$) may be joined along a circle to comprise a fundamental domain; the asymptotes coincide at $r_* = 3/5$ as in the proof of Lemma 11 below.

Thus, we obtain a first integral

$$\frac{r}{\sqrt{(r'^2+r^2+1)(r^2+1)}} + \frac{H_s}{r^2+1} = c. \tag{28}$$

Changing variables in (25), we obtain

$$r\theta'' = -\operatorname{sign}(\theta')2H_s r\left(\theta'^2 + \frac{1}{r^2+1}\right)^{3/2} - \frac{1}{r^2+1}\theta' + (r^2-1)\theta'^3.$$

At this point, we recall that the formula (25) assumes the outward normal on an annular piece of surface, and if θ' changes sign at a smooth finite point of the curve traced out by (r, θ), then Equation (25) is using the opposite choice of normal on opposite sides of that sign change. If $\theta'(r) > 0$ for $r < r_0$, for example, with

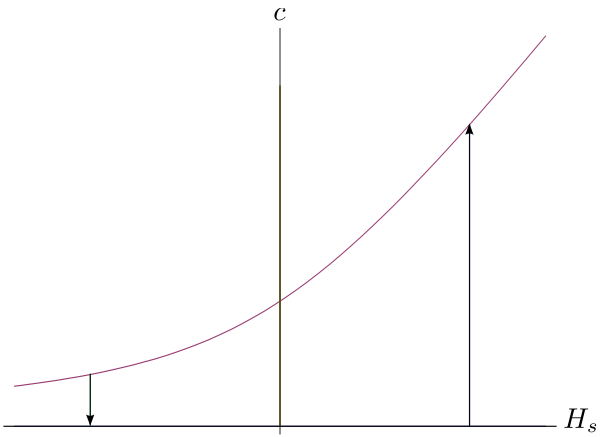

Figure 13. Piecing together solutions represented in parameter space.

$\theta'(r) > 0$ for $r > r_0$, then the equation above assumes the downward (that is, outward) normal for $r < r_0$ and the upward (that is, outward) normal for $r > r_0$. Taking this into account, we get a single equation applying to a single CMC annulus having mean curvature H_s with respect to the upward normal (that is, in the positive θ direction), which is nonsingular with respect to the parameterization (27):

$$r\theta'' = 2H_s r\left(\theta'^2 + \frac{1}{r^2+1}\right)^{3/2} - \frac{1}{r^2+1}\theta' + (r^2-1)\theta'^3. \tag{29}$$

This is the origin of Equation (3), which we could have derived from the parameterization itself via a long calculation. The first integral proved more difficult to derive for this equation as well.

The same change of variables in (28) yields

$$\theta'^2 = \frac{(cr+(c-H_s)/r)^2}{(r^2+1)(1-(cr+(c-H_s)/r)^2)}. \tag{30}$$

It is easily checked that this agrees with (4) up to a sign. In fact, consideration of both possible signs only results in obtaining geometrically congruent pieces of surface, as we will explain below.

The expression on the right in (30) is well defined on intervals where the function $f(r) = cr + (c - H_s)/r$ takes values in $(-1, 1)$. Furthermore, if we temporarily ignore the possibility of ambiguity due to a sign change when f vanishes, we can take the square root in (30) and obtain

$$\theta' = \frac{f}{\sqrt{(r^2+1)(1-f^2)}}, \tag{31}$$

where we have ignored the possible sign change of the right side, since that is equivalent to a change in sign of both c and H_s. It is straightforward to see that the right side has integrable singularities at values of r_m for which $f(r_m) = \pm 1$. A very simple analysis of this function f (see Figure 14) leads to the distinct parameter regions of Theorem 1 and a complete qualitative understanding of the (θ, r) meridian curves for solutions, as summarized in the following result, which we state for convenience under the temporary restriction $c \geq 0$.

Lemma 7. *Let $r \mapsto (\theta(r), r)$ parameterize a portion of the meridian curve of a CMC surface satisfying (31) with $c \geq 0$. The inclination angle ψ of such a curve with respect to the r-axis satisfies*

$$\sin\psi := \frac{\theta'}{\sqrt{1+\theta'^2}} = \frac{f}{\sqrt{1+r^2(1-f^2)}}.$$

Consequently, $\sin\psi$ *has the same monotonicity and sign of f on their common interval of definition. Furthermore, they both take the values ± 1 at precisely the same singular values r_m. The qualitative behavior of* $\sin\psi$ *may thus be obtained from that of f as follows*:

(i) *If $c = 0$ and $H_s > 0$, then* $\sin\psi$ *takes the value -1 at $r_{\min} = H_s$ and increases to 0 smoothly on the interval $[r_{\min}, \infty)$. The singularity is integrable and the resulting solution is a catenoid-type surface described by Theorem 1*(iii).

(ii) *If $0 < c < H_s$, then* $\sin\psi = -1$ *at $r_{\min} = (-1 + \sqrt{1 - 4c(c - H_s)})/(2c)$ and increases to $+1$ at $r_{\max} = (1 + \sqrt{1 - 4c(c - H_s)})/(2c)$. Both singularities are integrable, and the resulting solution is of nodoid-type as described by Theorem 1*(v).

(iii) *If $0 < c = H_s$, then $f(r) = cr$, and* $\sin\psi$ *is defined on $[0, 1/c]$ with an integrable singularity at $1/c$. Elementary integration leads to the spherical surfaces described in Theorem 1*(i); *the case $c = H_s = 0$ is also described there.*

(iv) *If $c - 1/(4c) < H_s < c$, then* $\sin\psi$ *is positive and well defined precisely between the singular points $r_{\min} = (1 - \sqrt{1 - 4c(c - H_s)})/(2c)$ and $r_{\max} = (1 + \sqrt{1 - 4c(c - H_s)})/(2c)$; at both of these points* $\sin\psi = +1$. *Again, both singularities are integrable, and one obtains a solution with profile curve of unduloid-type as in Theorem 1*(iv).

This lemma is essentially self-explanatory. One can almost obtain Theorem 1 directly from this result by simply expressing the integrals for θ in terms of standard elliptic integrals. The only ambiguities arise from various questions concerning signs, which we now discuss.

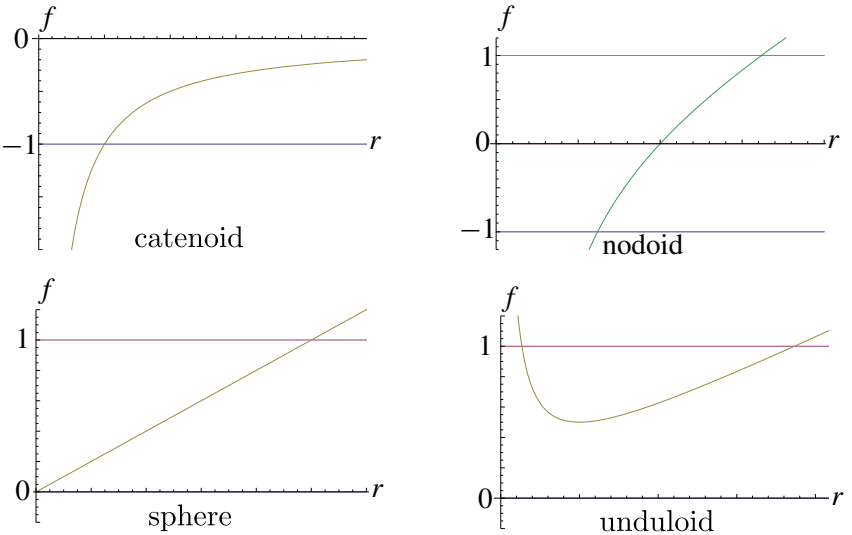

Figure 14. Profiles of inclination angle/indicator function f.

We recall that the only ambiguity in taking the square root in (30) is when f changes sign. This only occurs in the case of nodoid-type surfaces. When that sign change occurs, one has $\theta'' \neq 0$, that is, nodoid-type meridians have no inflections. Thus, the uniqueness theorem for ODEs applied to Equation (29) shows that one must keep the same sign across the singularity. This justifies only consideration of (31) as long as we consider all possible signs for c and H_s.

Our classification does not, in fact, consider all possible signs for c and H_s, because the surface corresponding to (H_s, c) is geometrically congruent to the $(-H_s, -c)$ surface. For example, if $c = 0 > H_s$, we obtain a surface geometrically congruent to that for $c = 0 < H_s$, but with stereographic projection reflected across a plane through the z-axis; this is simply a change of sign for H_s corresponding to a reversal of normal as described in connection with Equation (29). The same remarks apply to all pairs of surfaces determined by the correspondence $(H_s, c) \longleftrightarrow (-H_s, -c)$.

We conclude this section with some remarks on the reduction to standard elliptic integrals and the resulting period conditions.

For catenoid-type surfaces ($c = 0$, $H_s > 0$), we have

$$\theta(r) = -H_s \int_{H_s}^{r} \frac{1}{\sqrt{(\tau^2+1)(\tau^2-H_s^2)}}\, d\tau.$$

(Technically, $|\theta'(r_0)| < \infty$ implies $r(0) = r_0 > H_s$, but since the singularity at H_s is integrable, we may apply a rotation R^{xy} to obtain the expression above.) The

change of variables $\tau = H_s \sec t$ yields

$$\begin{aligned}\theta(r) &= -H_s \int_0^{\cos^{-1}(H_s/r)} \frac{\sec t}{\sqrt{H_s^2 \sec^2 t + 1}}\, dt \\ &= -\cos\alpha\, F(\cos^{-1}(H_s/r), \alpha), \end{aligned} \tag{32}$$

where $\alpha = \sin^{-1}(1/\sqrt{H_s^2+1})$ and $F(\phi,\alpha) = \int_0^\phi 1/\sqrt{1-\sin^2\alpha\sin^2 t}\, dt$ is the standard elliptic integral of the first kind.

Thus one finds, as described in Theorem 1(iii), that $\theta_{\max} = \cos\alpha\, K(\alpha)$, where $K(\alpha) = F(\pi/2,\alpha)$ is the complete elliptic integral of the first kind. One can show that $\theta_{\max}$ increases as a function of H_s, taking all values between 0 and $\pi/2$. While the general properties of elliptic integrals are well known, it can be somewhat involved to verify statements like these. For brevity, we will only show how one such result is proved and leave the rest to precisely stated lemmas involving one-dimensional calculus, accompanied by illustrative numerical plots.

Lemma 8. *The function* $\cos\alpha\, K(\alpha)$ *is decreasing in* α *with*

$$\lim_{\alpha\searrow 0} \cos\alpha\, K(\alpha) = \pi/2 \quad \textit{and} \quad \lim_{\alpha\nearrow \pi/2} \cos\alpha\, K(\alpha) = 0.$$

Proof. Note first that $(d/d\alpha)K = \sec\alpha\csc\alpha\, E - \cot\alpha\, K$, where

$$E(\phi,\alpha) = \int_0^\phi \sqrt{1-\sin^2\alpha\sin^2 t}\, dt$$

is the standard elliptic integral of the second kind and (here) $E = E(\alpha) = E(\pi/2,\alpha)$ is the complete elliptic integral of the second kind [Whittaker and Watson 1996, page 521]. Thus,

$$\begin{aligned}\frac{d}{d\alpha}(\cos\alpha\, K) &= -\sin\alpha\, K + \csc\alpha\, E - \cos\alpha\cot\alpha\, K = \frac{1}{\sin\alpha}(E-K) \\ &= -\int_0^{\pi/2} \frac{\sin\alpha\sin^2 t}{\sqrt{1-\sin^2\alpha\sin^2 t}}\, dt < 0.\end{aligned}$$

The first limit is immediate. To see the second, observe that for any $\epsilon \in (0,1)$, there is some $\delta = \delta(\epsilon) > 0$ such that $\sin^2 t \le 1-(1-\epsilon)(t-\pi/2)^2$ for $\pi/2-\delta \le t \le \pi/2$. Consequently,

$$\begin{aligned}\cos\alpha\, K &= \cos\alpha\left(\int_0^{\pi/2-\delta} \frac{1}{\sqrt{1-\sin^2\alpha\sin^2 t}}\, dt + \int_{\pi/2-\delta}^{\pi/2} \frac{1}{\sqrt{1-\sin^2\alpha\sin^2 t}}\, dt\right) \\ &\le \cos\alpha \int_0^{\pi/2-\delta} \sec t\, dt + \int_{\pi/2-\delta}^{\pi/2} \frac{\cos\alpha}{\sqrt{1-\sin^2\alpha(1-(1-\epsilon)(t-\pi/2)^2)}}\, dt\end{aligned}$$

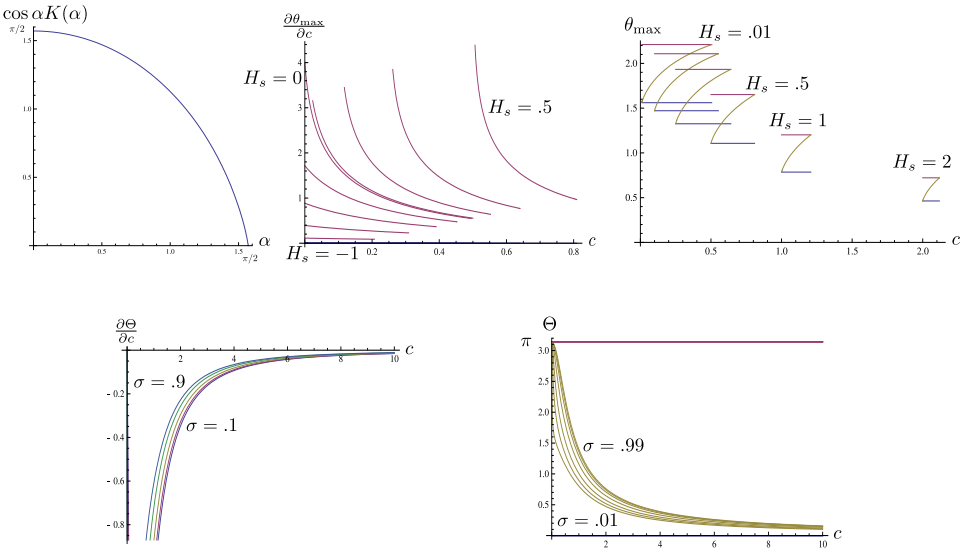

Figure 15. Properties of elliptic integrals.

$$
\begin{aligned}
&= \cos\alpha \int_0^{\pi/2-\delta} \sec t\, dt + \int_0^{\delta} \frac{\cos\alpha}{\sqrt{\cos^2\alpha + \sin^2\alpha(1-\epsilon)t^2}}\, dt \\
&= \cos\alpha \int_0^{\pi/2-\delta} \sec t\, dt + \int_0^{\delta} \frac{\cot\alpha/\sqrt{1-\epsilon}}{\sqrt{\cot^2\alpha/(1-\epsilon) + t^2}}\, dt \\
&= \cos\alpha \int_0^{\pi/2-\delta} \sec t\, dt + \frac{\cot\alpha}{\sqrt{1-\epsilon}} \left(\ln\left(\delta + \sqrt{\frac{\cot^2\alpha}{1-\epsilon} + \delta^2}\right) - \ln\left(\sqrt{\frac{\cot^2\alpha}{1-\epsilon}}\right)\right).
\end{aligned}
$$

Since ϵ is fixed in $(0, 1)$ and δ is fixed and positive,

$$
\lim_{\alpha\nearrow\pi/2} \cos\alpha K = -\lim_{\alpha\nearrow\pi/2} \cot\alpha \ln(\cos\alpha)/\sqrt{1-\epsilon} = 0. \qquad \square
$$

It is essentially the same for reductions of unduloid-type ($c - 1/(4c) < H_s < c$) and nodoid-type ($0 < c < H_s$). In each case, we may take $r_0 = r_{\min}$, so that

$$
\begin{aligned}
\theta(r) &= \frac{1}{c} \int_{r_{\min}}^{r} \frac{c(\tau^2+1) - H_s}{\sqrt{(1+\tau^2)(r_{\max}^2 - \tau^2)(\tau^2 - r_{\min}^2)}}\, d\tau \\
&= \frac{c - H_s}{c} \int_{r_{\min}}^{r} \frac{1}{\sqrt{(1+\tau^2)(r_{\max}^2 - \tau^2)(\tau^2 - r_{\min}^2)}}\, d\tau \\
&\qquad + \int_{r_{\min}}^{r} \frac{\tau^2}{\sqrt{(1+\tau^2)(r_{\max}^2 - \tau^2)(\tau^2 - r_{\min}^2)}}\, d\tau.
\end{aligned}
$$

In each integral we substitute

$$t = \sin^{-1}\sqrt{1-(r_{\min}/\tau)^2/(1-\mu^2)},$$

where $\mu = r_{\min}/r_{\max} \in (0,1)$ and obtain

$$\tau = \frac{r_{\min}}{\sqrt{1-(1-\mu^2)\sin^2 t}}, \qquad d\tau = \frac{(1-\mu^2)r_{\min}\sin t\cos t}{(1-(1-\mu^2)\sin^2 t)^{3/2}},$$

$$\frac{1}{\sqrt{1+\tau^2}} = \frac{\sqrt{1-(1-\mu^2)\sin^2 t}}{\sqrt{1-(1-\mu^2)\sin^2 t + r_{\min}^2}}$$

$$= \frac{1}{\sqrt{1+r_{\min}^2}}\cdot\frac{\sqrt{1-(1-\mu^2)\sin^2 t}}{\sqrt{1-(1-\mu^2)\sin^2 t/(1+r_{\min}^2)}},$$

$$\frac{1}{\sqrt{r_{\max}^2-\tau^2}} = \frac{\sqrt{1-(1-\mu^2)\sin^2 t}}{r_{\max}\cos t\sqrt{1-\mu^2}}, \qquad \frac{1}{\sqrt{\tau^2-r_{\min}^2}} = \frac{\sqrt{1-(1-\mu^2)\sin^2 t}}{r_{\min}\sin t\sqrt{1-\mu^2}},$$

so that

$$\theta(r) = \frac{c-H_s}{cr_{\max}\sqrt{1+r_{\min}^2}}\int_0^A \frac{1}{\sqrt{1-(1-\mu^2)\sin^2 t/(1+r_{\min}^2)}}\,dt$$

$$+ \frac{\mu r_{\min}}{\sqrt{1+r_{\min}^2}}\int_0^A \frac{1}{(1-(1-\mu^2)\sin^2 t)\sqrt{1-(1-\mu^2)\sin^2 t/(1+r_{\min}^2)}}\,dt$$

$$= \frac{c-H_s}{cr_{\max}d_0}F(A,\alpha) + \frac{\mu r_{\min}}{d_0}\Pi(\nu, A, \alpha)$$

where

$$A = \sin^{-1}\sqrt{\frac{1-(r_{\min}/r)^2}{1-\mu^2}}, \qquad d_0 = \sqrt{1+r_{\min}^2},$$

$$\alpha = \sin^{-1}\frac{\sqrt{1-\mu^2}}{d_0} = \sin^{-1}(\sqrt{\nu}/d_0), \qquad \nu = 1-\mu^2,$$

and

$$\Pi(\nu,\phi,\alpha) = \int_0^\phi \frac{1}{(1-\nu\sin^2 t)\sqrt{1-\sin^2\alpha\sin^2 t}}\,dt$$

is the standard elliptic integral of the third kind.

For both the unduloid and nodoid-type surfaces, the half-period

$$\theta(r_{\max}) = \frac{c-H_s}{cr_{\max}d_0}K(\alpha) + \frac{\mu r_{\min}}{d_0}\Pi(\nu, \pi/2, \alpha) \tag{33}$$

is of interest. Let us first consider the unduloid-type region by fixing H_s and restricting attention to vertical segments $\max\{0, H_s\} < c < (H_s + \sqrt{H_s^2+1})/2$.

Lemma 9. *For fixed H_s, the function $\theta_{\max} = \theta(r_{\max})$ is increasing as a function of c on* $(\max\{0, H_s\}, (H_s + \sqrt{H_s^2+1})/2)$ *with*

$$\lim_{c \searrow \max\{0,H_s\}} \theta_{\max} = \begin{cases} \dfrac{\pi}{2} - \dfrac{H_s}{\sqrt{H_s^2+1}} K\left(\sin^{-1}(1/\sqrt{H_s^2+1})\right) & \text{if } H_s < 0, \\ \sin^{-1}(1/\sqrt{H_s^2+1}) & \text{if } H_s \geq 0 \end{cases}$$

and

$$\lim_{c \nearrow \left(H_s+\sqrt{H_s^2+1}\right)/2} \theta_{\max} = \frac{\sqrt{H_s^2+1} - H_s}{\sqrt{2\left(H_s^2+1-H_s\sqrt{H_s^2+1}\right)}}\,\pi.$$

Notes on proof. The derivative $\partial\theta_{\max}/\partial c$ is a (complicated) expression of the form $AK(\alpha)+BE(\alpha)$, where K and E are the complete elliptic integrals of the first and second kinds, and A and B are rational functions of c, H_s, and $\sqrt{1-4c(c-H_s)}$. The second plot in Figure 15 shows the values of this derivative as a function of c in the unduloid-type region for $H_s = -1, -.5, -.25, -.1, -.01, 0, .1, .25, .5$.

In order to see the limits, it is convenient to set $\lambda = \sqrt{1-4c(c-H_s)}$ and write, for example, $r_{\min}$ and d_0 in the nonsingular forms

$$r_{\min} = \frac{2(c-H_s)}{1+\lambda} \quad \text{and} \quad d_0 = \frac{\sqrt{(1+\lambda)^2+4(c-H_s)^2}}{1+\lambda} = \frac{\sqrt{2}\sqrt{1+\lambda-2H_s(c-H_s)}}{1+\lambda}.$$

Making these substitutions, it is not difficult to see that

$$\frac{c-H_s}{cr_{\max}d_0}K(\alpha) = \frac{\sqrt{2}(c-H_s)}{\sqrt{1+\lambda-2H_s(c-H_s)}}K\left(\sin^{-1}\sqrt{\frac{2\lambda}{1+\lambda-2H_s(c-H_s)}}\right)$$

and

$$\frac{\mu r_{\min}}{d_0}\Pi(\nu, \pi/2, \alpha) = \frac{\sqrt{2}(c-H_s)(1-\lambda)}{(1+\lambda)\sqrt{1+\lambda-2H_s(c-H_s)}}\Pi\left(\frac{4\lambda}{(1+\lambda)^2}, \pi/2, \sin^{-1}\sqrt{\frac{2\lambda}{1+\lambda-2H_s(c-H_s)}}\right).$$

The sum of these two expressions is, of course, $\theta(r_{\max})$; it is convenient to refer to the first one as the "K part" and the second one as the "Π part."

When $H_s < 0$ is fairly straightforward to see that

$$\lim_{c\searrow 0}\frac{c-H_s}{cr_{\max}d_0}K(\alpha) = -\frac{H_s}{\sqrt{H_s^2+1}}K\left(\sin^{-1}\left(\frac{1}{\sqrt{H_s^2+1}}\right)\right).$$

The term in (33) involving an elliptic integral of the third kind (the Π part) is more difficult for this limit. One finds, from the fact that $H_s < 0$, that for c small the integral falls into the circular classification with $\sin^2\alpha < \nu < 1$ according to Milne-Thompson [Abramowitz and Stegun 1964]. It follows that

$$\Pi(\nu, \pi/2, \alpha) = K(\alpha) + (\pi/2)\delta_2(1 - \Lambda_0(\phi, \alpha)),$$

where $\delta_2 = \sqrt{\nu/((1-\nu)(\nu - \sin^2\alpha))}$ and Λ_0 is Heuman's lambda function with $\phi = \sin^{-1}\sqrt{(1-\nu)/\cos^2\alpha}$. Thus, from the expression above, one sees that it is only necessary to compute

$$\lim_{c\searrow 0}(1-\lambda)(K(\alpha) + (\pi/2)\delta_2(1 - \Lambda_0(\phi, \alpha))).$$

It is easily checked that $(1-\lambda)/\cos\alpha$ has a finite limit, so that Lemma 8 applies to the first term. One can next see that the limit in the last argument of Λ_0 is nonsingular, so that one need only consider

$$\lim_{\lambda\nearrow 1}(1-\lambda)\delta_2(1 - \Lambda_0(\phi, \alpha_0))\pi \quad \text{where } \alpha_0 = \sin^{-1}(1/\sqrt{H_s^2+1}).$$

Since Λ_0 is finite valued at $\phi = 0$ for all fixed α_0, one only needs to check that the finite value taken by δ_2 in the limit (with $\nu = 4\lambda/(1+\lambda)^2$) is the correct one.

It is interesting that the limit of $\theta_{\max}$ is singular for $H_s < 0$ and $c \searrow 0$: Comparing to the catenoid-type surfaces that correspond to $H_s < 0 = c$, we might expect the value $-\cos\alpha_0 K(\alpha_0)$ in accord with (32), and this is attained by the limit of the K part. An additional contribution of $\pi/2$ arises from the limit of the Π part. Thus, considering the convergence of the generating curves, the portion of the generating curve left of the inflection is dominated by the K part and that to the right is dominated by the Π part.

The second and third limits are both represented in the third graph of Figure 15. As the unduloid-type surfaces approach spheres, the limit is nonsingular; the K part vanishes in the limit and the Π part gives the value $\sin^{-1}(1/\sqrt{H_s^2+1})$ indicated.

The third (upper) limit is nonsingular and straightforward since λ tends to zero as the unduloid-type surfaces approach the standard tori. There is a peculiarity to our expressions in Theorem 1: In this limit, our expression for $r_{\min}$ (and the one for $r_{\max}$) tends to $(\sqrt{H_s^2+1} - H_s)/2$, apparently at odds with Theorem 1(iv). For convenience, we considered the tori with respect to the outward normal and the unduloid-type surfaces with respect to the inward normal; note that reversing the sign of H_s harmonizes the classification. □

Next, we consider the same region by fixing $\sigma \in (0, 1)$ and restricting attention to the curve

$$H_s = c - (1-\sigma)/(4c),$$

as indicated in Figure 16. Thus, we write $\Theta(\sigma, c) := \theta_{\max}(c - (1-\sigma)/(4c), c)$.

Lemma 10. *For $\sigma \in (0, 1)$ fixed, Θ is a decreasing function of c with*

$$\lim_{c\searrow 0}\Theta = \pi \quad \textit{and} \quad \lim_{c\nearrow\infty}\Theta = 0.$$

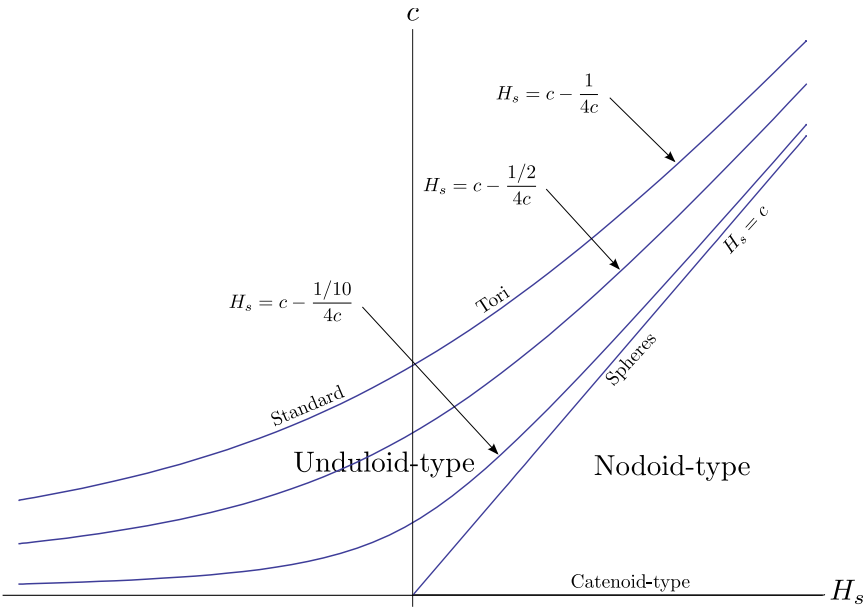

Figure 16. Curves that foliate the parameter region $c - 1/(4c) < H_s < c$.

Notes on the proof. We see immediately that $\lambda = \sqrt{\sigma}$ so that

$$\frac{c - H_s}{c r_{\max} d_0} K(\alpha) = \frac{1 - \sqrt{\sigma}}{\sqrt{4c^2 + (1-\sqrt{\sigma})^2}} K\left(\sin^{-1}\left(\frac{4c}{1+\sqrt{\sigma}}\sqrt{\frac{\sqrt{\sigma}}{4c^2 + (1-\sqrt{\sigma})^2}}\right)\right)$$

and

$$\frac{\mu r_{\min}}{d_0}\Pi(\nu, \pi/2, \alpha) = \frac{(1-\sqrt{\sigma})^2}{(1+\sqrt{\sigma})\sqrt{4c^2 + (1-\sqrt{\sigma})^2}} \times \Pi\left(\frac{4\sigma}{(1+\sqrt{\sigma})^2}, \pi/2, \sin^{-1}\left(\frac{4c}{1+\sqrt{\sigma}}\sqrt{\frac{\sqrt{\sigma}}{4c^2 + (1-\sqrt{\sigma})^2}}\right)\right).$$

Note that the c dependence is not as complicated in this case. The derivative $\partial\Theta/\partial c$ has the form $AK(\alpha) + BE(\alpha)$, with A and B rational functions of σ, c, and $\sqrt{4c^2 + (1-\sqrt{\sigma})^2}$. The fourth graph in Figure 15 gives $\partial\Theta/\partial c$ for various values of σ. The fifth graph illustrates the limits. □

Corollary 3. (i) *For each $m = 2, 3, \ldots$ and $\sigma \in (0, 1)$ fixed, there is a unique $c = c_m(\sigma)$ for which $\Theta(\sigma, c_m) = \pi/m$.*

(ii) $\dfrac{\partial\theta_{\max}}{\partial H_s} < 0.$

(iii) *The condition $\theta_{\max}(H_s, c) = \pi/m$ defines smooth curves, as indicated in Theorem 1.*

Proof. The first claim is immediate from the monotonicity of the preceding lemma. The second follows from differentiation:

$$\frac{\partial\Theta}{\partial\sigma}(\sigma, c) = \frac{\partial\theta_{\max}}{\partial H_s}(c - \frac{1-\sigma}{4c}, c) \cdot \frac{1}{4c}.$$

The third follows from the second, since we obtain the ODE

$$\frac{\partial\theta_{\max}}{\partial H_s}(H_s, c_m) + \frac{\partial\theta_{\max}}{\partial c}(H_s, c_m)c_m' = 0. \qquad \square$$

Qualitatively, we observe for nodoid-type surfaces that the loops in the generating curve always face the θ-axis. More precise is the following result, whose proof is similar to the one found in [Hynd and McCuan 2006].

Lemma 11. *If* $0 < c < H_s$, *then* $\theta(r_{\max}) > \theta(r_{\min})$.

Proof. With the normalization $\theta_{\min} = 0$ as above, this assertion is equivalent to $\theta(r_{\max}) > 0$. To see this, we return to the expression (31). Notice that $f(r) = cr + (c - H_s)/r$ is increasing and concave on $[r_{\min}, r_{\max}]$, taking values -1 and 1 at the endpoints. We let $r_* = \sqrt{H_s/c - 1}$ denote the unique zero of f. Setting $\tau(r) = (H_s - c)/(cr)$, which is the unique solution of $f(\tau) = -f(r)$, we find

$$\begin{aligned}\theta(r_{\max}) &= \int_{r_{\min}}^{r_*} \frac{f}{\sqrt{(r^2+1)(1-f^2)}}\,dr + \int_{r_*}^{r_{\max}} \frac{f}{\sqrt{(r^2+1)(1-f^2)}}\,dr \\ &= \int_{r_*}^{r_{\max}} \frac{1}{r}\left(\frac{r}{\sqrt{r^2+1}} - \frac{(H_s-c)/(cr)}{\sqrt{((H_s-c)/(cr))^2+1}}\right)\frac{f}{\sqrt{1-f^2}}\,dr.\end{aligned}$$

Notice that $r/\sqrt{r^2+1}$ is increasing, and that $r \geq (H_s - c)/(cr)$ when $r \geq r_* = \sqrt{(H_s - c)/c}$. Thus, $\theta_{\max} > 0$. $\square$

3. Spherically symmetric compact surfaces

We now consider the more general condition of spherical symmetry and prove Theorem 2. Let $\mathcal{S} \subset \mathbb{S}^3$ be a compact surface with spherical symmetry.

Recall our discussion of spherical symmetry in Section 1.2 and the fact that stereographic projection extends naturally to $\mathbb{R}^4 \setminus \{x_4 = 1\}$. We begin with the preliminary rotation described there, which resulted in $\Lambda^* = \{-a_0\mathbf{e}_1 + t\mathbf{e}_3 : t \in \mathbb{R}\}$ with $a_0 > 1$. If, having made this normalization, we have that $\mathbf{e}_4 \notin \mathcal{S}$, then

$$\mathcal{P} = \pi(\mathcal{S}) \textit{ is a compact surface in } \mathbb{R}^3 \textit{ with spherical symmetry along a line.}$$

Otherwise, we seek to find a preliminary rotation R so that this assertion is true of $\mathcal{P} = \pi(R(\mathcal{S}))$. Using once again [Hirsch 1994, Proposition 3.1.2], we know that any neighborhood of $\mathbf{e}_4$ contains points of $\mathbb{S}^3 \setminus \mathcal{S}$. Taking such a point $\boldsymbol{p}$ and denoting its fourth coordinate by $\cos\epsilon$, we see that for some (small) rotation R_0

of $\mathbb{R}^3$, we can arrange to have $R_0^{-1} \circ R^{xw}_{-\epsilon}\mathbf{e}_4 = \boldsymbol{p}$. Thus, applying $R^{xw}_{\epsilon} \circ R_0$ as an additional preliminary rotation, we may assume

$$\Lambda^* = \{R^{xw}_{\epsilon}(-a_0 R_0(\mathbf{e}_1) + t\, R_0(\mathbf{e}_3)) : t \in \mathbb{R}\}.$$

We may write

$$R_0(\mathbf{e}_1) = \sum a_{1j}\mathbf{e}_j \quad \text{and} \quad R_0(\mathbf{e}_3) = \sum a_{3j}\mathbf{e}_j$$

so that

$$\begin{aligned}\lambda(t) &= R^{xw}_{\epsilon}(-a_0 R_0(\mathbf{e}_1) + t\, R_0(\mathbf{e}_3)) \\ &= (-a_0 a_{11} + t a_{31})\cos\epsilon\,\mathbf{e}_1 + \sum_{j=2}^{3}(-a_0 a_{1j} + t a_{3j})\mathbf{e}_j + (-a_0 a_{11} + t a_{31})\sin\epsilon\,\mathbf{e}_4.\end{aligned}$$

Since $|a_{11}| \le 1$ and is fixed, we may assume ϵ is small enough so $-a_0 a_{11}\sin\epsilon \ne 1$. It follows that there is at most one value of t for which $\lambda(t)$ can intersect the plane $\{x_4 = 1\}$. More precisely, if $a_{31} = 0$, then $\Lambda^* \cap \{x_4 = 1\} = \phi$ and the reasoning of Section 1.2 yields that $\pi(\mathcal{S} \setminus \{\mathbf{e}_4\}) = \pi(\mathcal{S})$ is a compact surface with spherical symmetry along the line $L = \pi(\Lambda^*)$. If $a_{31} \ne 0$, then $\lambda(t_0) \in \{x_4 = 1\}$ for the unique value $t_0 = (1 + a_0 a_{11}\sin\epsilon)/(a_{31}\sin\epsilon)$. We pause here to relabel so that $\Lambda^* = \{\boldsymbol{b} + t\boldsymbol{v} : t \in \mathbb{R}\}$ with $(\boldsymbol{b} + t\boldsymbol{v})\cdot\mathbf{e}_4 \ne 1$ unless $t = t_0$. Setting $\boldsymbol{b} = (b_1, b_2, b_3, b_4)$, $\boldsymbol{v} = (v_1, v_2, v_3, v_4)$, $\underline{\boldsymbol{b}} = (b_1, b_2, b_3)$ and $\underline{\boldsymbol{v}} = (v_1, v_2, v_3)$ as usual, we have for $t \ne t_0$

$$\pi(\boldsymbol{b} + t\boldsymbol{v}) = \frac{\underline{\boldsymbol{b}} + t\underline{\boldsymbol{v}}}{1 - (b_4 + t v_4)} = \frac{1}{1 - b_4}\underline{\boldsymbol{b}} + \frac{t}{1 - (b_4 + t v_4)}\left(\frac{v_4}{1 - b_4}\underline{\boldsymbol{b}} + \underline{\boldsymbol{v}}\right).$$

Thus, $\mathcal{P} = \pi(\mathcal{S})$ is a compact immersed surface in $\mathbb{R}^3$ which, by our discussion of radial lines, is invariant under maps

$$\psi(\boldsymbol{x}) = \rho^2 \frac{\boldsymbol{x} - \boldsymbol{a}}{|\boldsymbol{x} - \boldsymbol{a}|^2} + \boldsymbol{a},$$

where

$$\boldsymbol{a} = \boldsymbol{a}(t) = \frac{1}{1 - b_4}\underline{\boldsymbol{b}} + \frac{t}{1 - (b_4 + t v_4)}\left(\frac{v_4}{1 - b_4}\underline{\boldsymbol{b}} + \underline{\boldsymbol{v}}\right) \quad \text{for } t \in \mathbb{R} \setminus \{t_0\}$$

and $\rho = \rho(t) > 0$. The centers of reflection $\boldsymbol{a}(t)$ include all points on a line L in $\mathbb{R}^3$ except $\boldsymbol{a}_1 = \lim_{t\to\infty}\boldsymbol{a}(t) = -\underline{\boldsymbol{v}}/v_4$. We now recall that $\mathbf{e}_4 + \boldsymbol{v}/|\boldsymbol{v}| \in \bigcup_{\ell^* \in \mathcal{R}} \ell^*$. Therefore, some radial line contains $\mathbf{e}_4 + \boldsymbol{v}/|\boldsymbol{v}|$, and there is some sphere $\partial B_\rho(\boldsymbol{a}) \subset \mathbb{R}^3$ with center $\boldsymbol{a} = \pi(\mathbf{e}_4 + \boldsymbol{v}/|\boldsymbol{v}|) = -\underline{\boldsymbol{v}}/v_4 = \boldsymbol{a}_1$ about which $\mathcal{P}$ is symmetric. Thus, in all cases, it is possible after preliminary rotation to project a compact surface $\mathcal{S} \subset \mathbb{S}^3$ so that $\mathcal{P} = \pi(\mathcal{S})$ is compact in $\mathbb{R}^3$ and so that $\mathcal{P}$ has spherical symmetry along a line.

The reasoning above admits an additional preliminary rotation of $\mathbb{R}^3$, which we now use to again pause and relabel:

Theorem 5. *Given a compact, connected surface $\mathcal{P}$ immersed in $\mathbb{R}^3$ and with spherical symmetry along a line $L = \{-a\mathbf{e}_1 + t\mathbf{e}_3 : t \in \mathbb{R}\} \subset \mathbb{R}^3$, the surface $\mathcal{S} = \pi^{-1}(\mathcal{P}) \subset \mathbb{S}^3$ has special spherical symmetry.*

A number of lemmas follow, which together prove this result. For all of them, we fix notation as follows: The symmetry spheres along L are denoted by $\partial B_\rho(\boldsymbol{x}_0)$ with $\rho = \rho(t)$ corresponding to $\boldsymbol{x}_0 = -a\mathbf{e}_1 + t\mathbf{e}_3$. The collection of all such spheres is denoted by Σ, and we denote by Ψ the set of associated reflection maps

$$\psi(\boldsymbol{x}) = \rho^2 \frac{\boldsymbol{x} - \boldsymbol{x}_0}{|\boldsymbol{x} - \boldsymbol{x}_0|^2} + \boldsymbol{x}_0.$$

The claim of Theorem 5 is equivalent to showing that each such sphere passes through a particular horizontal circle $\{(x, y, h) : (x + a)^2 + y^2 = \rho_0^2\}$.

Lemma 12. *$\mathcal{P} \cap L = \phi$, and hence* $\operatorname{dist}(\mathcal{P}, L) > 0$.

Proof. If $\boldsymbol{x}_0 \in \mathcal{P} \cap L$, then there is a sequence of points $\boldsymbol{x}_j \in \mathcal{P} \setminus L$ with $\boldsymbol{x}_j \to \boldsymbol{x}_0$. Since

$$\lim_{j\to\infty} |\psi(\boldsymbol{x}_j)| = \lim_{j\to\infty} \left| \rho^2 \frac{\boldsymbol{x}_j - \boldsymbol{x}_0}{|\boldsymbol{x}_j - \boldsymbol{x}_0|^2} + \boldsymbol{x}_0 \right| \geq \lim_{j\to\infty} \left(\rho^2 \frac{1}{|\boldsymbol{x}_j - \boldsymbol{x}_0|} - |\boldsymbol{x}_0| \right) = \infty,$$

this contradicts compactness. □

Lemma 13. *For every $\boldsymbol{x}_0 \in L$, we must have $\mathcal{P} \cap \overline{B_\rho(\boldsymbol{x}_0)} \neq \phi$ and $\mathcal{P} \setminus B_\rho(\boldsymbol{x}_0) \neq \phi$.*

Proof. If $\boldsymbol{x} \in \mathcal{P} \setminus \overline{B_\rho(\boldsymbol{x}_0)}$, then $\psi(\boldsymbol{x}) \in \mathcal{P} \cap B_\rho(\boldsymbol{x}_0)$. □

Lemma 14. *$\mathcal{P}$ is symmetric with respect to a unique horizontal plane $L^\perp$ orthogonal to L.*

Proof. By compactness, there is some $R > 0$ such that $\mathcal{P} \subset B_R(-a\mathbf{e}_1)$. Consider $-a\mathbf{e}_1 + t_j\mathbf{e}_3$ with $t_j \nearrow +\infty$. When $t_j > R$, we must have $-a\mathbf{e}_1 + (t_j - \rho(t_j))\mathbf{e}_3$ on the segment connecting $-a\mathbf{e}_1 - R\mathbf{e}_3$ and $-a\mathbf{e}_1 + R\mathbf{e}_3$. Consequently, $-R \leq t_j - \rho(t_j) \leq R$. Taking a subsequence, we may assume $t_j - \rho(t_j) \to b_0 \in \mathbb{R}$ as $j \to +\infty$. For $\boldsymbol{x}$ in any compact set, such as $\mathcal{P}$,

$$\lim_{j\to\infty} \psi_j(\boldsymbol{x}) = \lim_{j\to\infty} \rho(t_j)^2 \frac{\boldsymbol{x} + a\mathbf{e}_1 - t_j\mathbf{e}_3}{|\boldsymbol{x} + a\mathbf{e}_1 - t_j\mathbf{e}_3|^2} - a\mathbf{e}_1 + t_j\mathbf{e}_3 = \boldsymbol{x} + 2(b_0 - \boldsymbol{x} \cdot \mathbf{e}_3)\mathbf{e}_3.$$

The last expression will be recognized as standard reflection with respect to the horizontal plane $L^\perp = \{x_3 = b_0\}$. This gives existence.

If there were another such plane of symmetry, the composition of the two associated reflections would provide a vertical translation to which $\mathcal{P}$ is invariant. This again contradicts the fact that $\mathcal{P}$ is bounded. □

Lemma 15. *Let $\psi, \tilde{\psi} \in \Psi$ with associated symmetry spheres $\partial B_\rho(\boldsymbol{x}_0)$, $\partial B_{\tilde{\rho}}(\tilde{\boldsymbol{x}}_0)$, both in Σ.*

(i) *$\partial B_\rho(\boldsymbol{x}_0)$ and $\partial B_{\tilde{\rho}}(\tilde{\boldsymbol{x}}_0)$ have nontrivial intersection outside of L.*

(ii) *$\partial B_\rho(\boldsymbol{x}_0)$ and $L^\perp$ have nontrivial intersection outside of L.*

(iii) *If $\boldsymbol{x}_0 \in \partial B_{\tilde\rho}(\tilde{\boldsymbol{x}}_0)$, then $\psi(\partial B_{\tilde\rho}(\tilde{\boldsymbol{x}}_0) \setminus \{\boldsymbol{x}_0\}) = L^\perp$.*

(iv) *If $\boldsymbol{x}_0 \notin \partial B_{\tilde\rho}(\tilde{\boldsymbol{x}}_0)$, then $\psi(\partial B_{\tilde\rho}(\tilde{\boldsymbol{x}}_0)) \in \Sigma$.*

Proof. For the first claim, we proceed by contradiction. If $\partial B_\rho(\boldsymbol{x}_0) \cap \partial B_{\tilde\rho}(\tilde{\boldsymbol{x}}_0) \subset L$, then either $B_\rho(\boldsymbol{x}_0) \subset B_{\tilde\rho}(\tilde{\boldsymbol{x}}_0)$, $B_{\tilde\rho}(\tilde{\boldsymbol{x}}_0) \subset B_\rho(\boldsymbol{x}_0)$, or $B_\rho(\boldsymbol{x}_0) \cap B_{\tilde\rho}(\tilde{\boldsymbol{x}}_0) = \phi$. The second possibility is (by relabeling) the same as the first. If the last possibility obtains, then a calculation shows that $\widetilde{\psi}(\partial B_\rho(\boldsymbol{x}_0))$ is a sphere $\partial B_{\bar\rho}(\bar{\boldsymbol{x}}_0))$ with $B_{\bar\rho}(\bar{\boldsymbol{x}}_0)) \subset B_{\tilde\rho}(\tilde{\boldsymbol{x}}_0)$. Also, a calculation shows that the reflection $\overline{\psi}$ associated with $\partial B_{\bar\rho}(\bar{\boldsymbol{x}}_0))$ is given by $\widetilde{\psi} \circ \psi \circ \widetilde{\psi}$. Thus, $\partial B_{\bar\rho}(\bar{\boldsymbol{x}}_0)) \in \Sigma$ and again the situation reduces to the first possibility $B_\rho(\boldsymbol{x}_0) \subset B_{\tilde\rho}(\tilde{\boldsymbol{x}}_0)$. We note for future reference that

$$\bar\rho = \frac{\tilde\rho^2 \rho}{|(t-\tilde t)^2 - \rho^2|} \quad \text{and} \quad \bar{\boldsymbol{x}}_0 = \tilde{\boldsymbol{x}}_0 + \frac{\tilde\rho^2}{(t-\tilde t)^2 - \rho^2}\mathbf{e}_3.$$

We begin with the special case $\boldsymbol{x}_0 = \tilde{\boldsymbol{x}}_0$. By the reasoning above (with $\boldsymbol{x}_0$ and $\tilde{\boldsymbol{x}}_0$ reversed), we obtain $\partial B_{\rho_1}(\boldsymbol{x}_0) \in \Sigma$ with $\rho_1 = \rho^2/\tilde\rho$. Repeating this construction with $B_{\rho_1}(\boldsymbol{x}_0)$ and $B_{\tilde\rho}(\boldsymbol{x}_0)$, we obtain $\partial B_{\rho_j}(\boldsymbol{x}_0) \in \Sigma$ with $\rho_j = \tilde\rho(\rho/\tilde\rho)^{2^j} \to 0$ since $\rho/\tilde\rho < 1$. According to Lemma 13, we must have points in $\mathcal{P}$ converging to $\boldsymbol{x}_0 \in L$. This contradicts Lemma 12. This special case has this corollary:

Corollary 4. *For each $\partial B_\rho(\boldsymbol{x}) \in \Sigma$, the radius $\rho = \rho(t)$ is uniquely determined.*

More generally, if $\partial B_\rho(\boldsymbol{x}_0)$ and $\partial B_{\tilde\rho}(\tilde{\boldsymbol{x}}_0)$ are not assumed to have the same center, but it is assumed that $\overline{B_\rho(\boldsymbol{x}_0)} \subset B_{\tilde\rho}(\tilde{\boldsymbol{x}}_0)$ so that $\delta = \operatorname{dist}(\partial B_\rho(\boldsymbol{x}_0), \partial B_{\tilde\rho}(\tilde{\boldsymbol{x}}_0)) > 0$, then the sequence of nested spheres $\partial B_{\rho_j}(\boldsymbol{x}_j) \in \Sigma$ may still be constructed as above, and from the formula for the radius, we see that

$$\rho_1 = \rho^2 \frac{\tilde\rho}{\tilde\rho + |\tilde t - t|} \cdot \frac{1}{\tilde\rho - |\tilde t - t|} \le \frac{\rho^2}{\rho + \delta} \le \rho.$$

Noting that $\overline{B_{\rho_1}(\boldsymbol{x}_1)} \subset B_{\tilde\rho}(\tilde{\boldsymbol{x}}_0)$ and $\delta_1 = \operatorname{dist}(\partial B_{\rho_1}(\boldsymbol{x}_1), \partial B_{\tilde\rho}(\tilde{\boldsymbol{x}}_0)) > \delta$, we find by induction (as follows) that

$$\begin{aligned}\rho_j &\le \rho_{j-1} \frac{\rho_{j-1}}{\tilde\rho - |\tilde t - t_{j-1}|} \\ &\le \rho \left(\frac{\rho}{\rho+\delta}\right)^{j-1} \frac{\rho_{j-1}}{\rho_{j-1}+\delta} \le \rho \left(\frac{\rho}{\rho+\delta}\right)^{j} \to 0 \quad \text{as } j \to +\infty.\end{aligned}$$

We again obtain arbitrarily small spheres and the same contradiction.

Finally, if $B_\rho(\boldsymbol{x}_0) \subset B_{\tilde\rho}(\tilde{\boldsymbol{x}}_0)$ with $\partial B_\rho(\boldsymbol{x}_0) \cap \partial B_{\tilde\rho}(\tilde{\boldsymbol{x}}_0) \neq \phi$, then making the same construction yields

$$\rho_1 = \frac{\rho^2 \tilde\rho}{\tilde\rho^2 - (\tilde\rho - \rho)^2} = \frac{\rho\tilde\rho}{2(\tilde\rho - \rho) + \rho}.$$

By induction in this case, we have

$$\rho_j = \frac{\rho\tilde{\rho}}{2^j(\tilde{\rho}-\rho)+\rho} \to 0 \quad \text{as } j \to +\infty,$$

and the contradiction is the same one. We have established the first assertion.

The second claim follows via contradiction from the first. If $B_\rho(\boldsymbol{x}_0) \cap L^\perp \subset L$, then $\psi(L^\perp) = \partial B_{\rho_1}(\boldsymbol{x}_1) \setminus \{\boldsymbol{x}_0\}$ with $\rho_1 < \rho$ and $B_{\rho_1}(\boldsymbol{x}_1) \subset B_\rho(\boldsymbol{x}_0)$. Also, letting ψ_0 denote reflection in $L^\perp$, and ψ_1 reflection in $\partial B_{\rho_1}(\boldsymbol{x}_1)$, we have $\psi_1 = \psi \circ \psi_0 \circ \psi$, at least outside of L. Thus, $\partial B_{\rho_1}(\boldsymbol{x}_1) \in \Sigma$ with $\partial B_{\rho_1}(\boldsymbol{x}_1) \cap \partial B_\rho(\boldsymbol{x}_0) \subset L$.

That $\psi(\partial B_{\tilde{\rho}}(\tilde{\boldsymbol{x}}_0) \setminus \{\boldsymbol{x}_0\})$ is a horizontal plane if $\boldsymbol{x}_0 \in \partial B_{\tilde{\rho}}(\tilde{\boldsymbol{x}}_0)$ follows from a calculation. Another shows that reflection with respect to that plane is given by $\psi \circ \widetilde{\psi} \circ \psi$ at all points in $\mathbb{R}^3 \setminus \{\boldsymbol{x}_0\}$. Since $\boldsymbol{x}_0 \notin \mathcal{P}$ by Lemma 12, we see that $\psi(\partial B_{\tilde{\rho}}(\tilde{\boldsymbol{x}}_0) \setminus \{\boldsymbol{x}_0\})$ is a symmetry plane for $\mathcal{P}$. This plane must be $L^\perp$ of course.

The last claim follows via a similar, and now familiar, reasoning. □

In view of the previous lemma, for each $\boldsymbol{x}_0 = -a\mathbf{e}_1 + t\mathbf{e}_3 \in L$ the radius $\rho_0(t)$ of the intersection circle of $\partial B_\rho(\boldsymbol{x}_0)$ with $L^\perp$ is well defined. The properties of this quantity are the key to the rest of the proof of Theorem 5.

Lemma 16. $\rho_0(t \pm \rho(t)) = \rho_0(t)$.

Proof. Let $\psi_\pm \in \Psi$ be the reflection associated to $\partial B_{\rho(t\pm\rho(t))}(\boldsymbol{x}_0 \pm \rho(t)\mathbf{e}_3) \in \Sigma$. Note that $\psi_\pm(\partial B_{\rho(t)}(\boldsymbol{x}_0) \setminus \{\boldsymbol{x}_0 \pm \rho(t)\})$ is a horizontal plane of symmetry for $\mathcal{P}$. By Lemma 14 that plane must be $L^\perp$. Moreover, the intersection circle $C_\pm = \partial B_{\rho(t\pm\rho(t))}(\boldsymbol{x}_0 \pm \rho(t)\mathbf{e}_3) \cap \partial B_{\rho(t)}(\boldsymbol{x}_0)$ is a nontrivial horizontal circle.

On the other hand, $C_\pm$ is fixed by $\psi_\pm$, and

$$\psi_\pm(C_\pm) \subset \psi_\pm(\partial B_{\rho(t)}(\boldsymbol{x}_0) \setminus \{\boldsymbol{x}_0 \pm \rho(t)\}) = L^\perp.$$

Thus $C_\pm \subset L^\perp$, and it follows that $C_\pm = \partial B_{\rho(t)}(\boldsymbol{x}_0) \cap L^\perp$. □

Lemma 17. $\rho_0(t) = \rho(b_0)$ *for every* $t \in \mathbb{R}$.

Proof. We again argue by contradiction. If for some t, we have $\rho_0(t_0) < \rho(b_0)$, then $\psi_{b_0}(\partial B_{\rho(t_0)}(-a\mathbf{e}_1 + t_0\mathbf{e}_3))$ is a sphere $\partial B_{\rho_1}(\boldsymbol{x}_1)$. As usual, $\partial B_{\rho_1}(\boldsymbol{x}_1) \in \Sigma$ and $\rho_0(t_1) > \rho(b_0)$.

Now we restrict attention to $t \in \mathbb{R}$ for which $\rho_0(t) = \rho_0(t_1)$. The previous lemma gives us many such t. We first observe that $\mathcal{B} = \{|t - b_0| : \rho_0(t) = \rho_0(t_1)\}$ is bounded away from zero. In fact, by the triangle inequality

$$|t - b_0| > \rho(t) - \rho_0(t) > \rho(t) - \rho(b_0) > 0.$$

On the other hand, setting $t_j = t_{j-1} + \rho(t_{j-1})$ for $j = 2, 3, \ldots$, we obtain a sequence with $\rho_0(t_j) = \rho_0(t_1)$ such that $|t_j - b_0| \in \mathcal{B}$. Also, since $\rho(t) > |t - b_0|$, we may assume $t_1 > b_0$. Then for $j \geq 2$, we have $t_j > 2t_{j-1} - b_0$, so that inductively we

find $t_j > 2^{j-1}t_1 - (2^{j-1}-1)b_0 = t_1 + (2^{j-1}-1)(t_1 - b_0) \to +\infty$ as $j \to +\infty$. It follows that $\rho(t_j) \to +\infty$ as $j \to +\infty$.

Finally, setting $\tau_j = t_j - \rho(t_j)$ we obtain another sequence of points with $\rho_0(\tau_j) = \rho_0(t_1) > \rho(b_0)$. These points satisfy

$$|\tau_j - b_0| = t_j - \tau_j - t_j + b_0 = \rho(t_j) - \sqrt{\rho(t_j)^2 - \rho_0(t_1)^2} \to 0 \quad \text{as } j \to +\infty.$$

This contradicts the fact that $\mathcal{B}$ is bounded away from zero. □

We have shown that every sphere $\partial B_\rho(\boldsymbol{x}_0)$ passes through the horizontal circle $\{(x, y, h) : (x+a)^2 + y^2 = \rho_0^2\}$ where $h = b_0$ and $\rho_0 = \rho(b_0)$. Thus, $\mathcal{S} = \pi^{-1}(\mathcal{P})$ has special spherical symmetry and Theorem 5 is proved. □

4. Rotational symmetry

If a nonspherical surface $\mathcal{S} \in \mathbb{S}^3$ stereographically projects to a surface of rotation about the projection of a geodesic, then we may assume the axis of symmetry in $\mathbb{R}^3$ is the z-axis and the meridian curve is given locally by $x = x(z)$. In this case, a natural parameterization for $\mathcal{P} = \pi(\mathcal{S})$ is

$$Y(\vartheta, z) = (x\cos\vartheta, x\sin\vartheta, z). \tag{34}$$

Stereographic projection of the expression in (2) yields

$$X(\theta, \phi) = (R\cos\theta, R\sin\theta, r\sin\phi), \quad \text{where } R = \sqrt{r^2+1} + r\cos\phi, \tag{35}$$

which does not, in general, have rotational symmetry in $\mathbb{R}^3$. Nevertheless, for an appropriate rotation R of $\mathbb{S}^3$, we find that $Y = \pi \circ R \circ \pi^{-1} \circ X$ does indeed have the form (34). In fact, taking $R = R^{yz}_{\pi/2} R^{xw}_{\pi/2}$, one checks easily that the resulting projected surface has all the planes passing through the z-axis as planes of symmetry. It follows that the surface is rotationally symmetric. Setting $\phi = 0$ and

$$z = \frac{(\sqrt{r^2+1}+r)(\sqrt{r^2+1}+r^2+1)\sin\theta}{\sqrt{r^2+1}+r^2+1+(\sqrt{r^2+1}+r)\cos\theta},$$

where $r = r(\theta, 0)$, we find the meridian curve is given by

$$x = \frac{(\sqrt{r^2+1}+r^2)(\sqrt{r^2+1}+r^2+1)}{\sqrt{r^2+1}+r^2+1+(\sqrt{r^2+1}+r)\cos\theta}.$$

We thus obtain the expression (34) parametrically in ϑ and θ:

$$Y = (x(\theta)\cos\vartheta, x(\theta)\sin\vartheta, z(\theta)).$$

Due to the spatial inhomogeneity of the spherical metric in $\mathbb{R}^3 = \pi(\mathbb{S}^3 \setminus \{\mathbf{e}_4\})$, it is not surprising that the meridian curves do not take a simple form. It is therefore

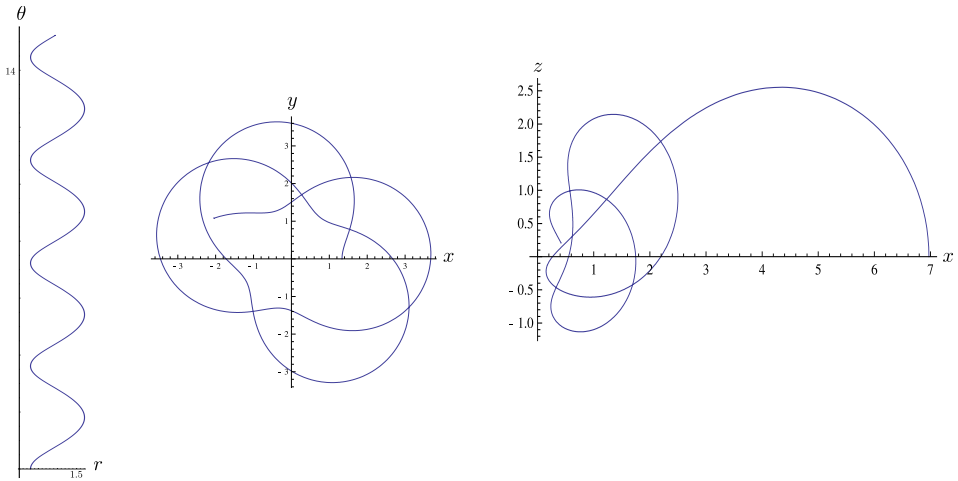

Figure 17. The generating curve of an unduloid-type surface, the stereographic projection of the curve $\phi = 0$ in Apollonian position, and the meridian of the same surface in symmetric position.

fortuitous that these surfaces are easily understood in terms of the (sometimes periodic) function r; the expression (35) might be called the *Apollonian form*.

We conclude with Figures 17–20, which are galleries of meridian curves of representative surfaces in rotationally symmetric form.

References

[Abramowitz and Stegun 1964] M. Abramowitz and I. A. Stegun, *Handbook of mathematical functions with formulas, graphs, and mathematical tables*, National Bureau of Standards Applied Mathematics Series **55**, Government Printing Office, 1964. MR 29 #4914 Zbl 0171.38503

[Alexandrov 1962] A. D. Alexandrov, "A characteristic property of spheres", *Ann. Mat. Pura Appl.* (4) **58** (1962), 303–315. MR 26 #722

[Brito and Leite 1990] F. Brito and M. L. Leite, "A remark on rotational hypersurfaces of S^n", *Bull. Soc. Math. Belg. Sér. B* **42**:3 (1990), 303–318. MR 91j:53028 Zbl 0734.53010

[do Carmo and Dajczer 1983] M. do Carmo and M. Dajczer, "Rotation hypersurfaces in spaces of constant curvature", *Trans. Amer. Math. Soc.* **277** (1983), 685–709. MR 85b:53055 Zbl 0518.53059

[Chern 1959] S. S. Chern, *Differentiable manifolds*, Textos de Matemática **4**, Instituto de Física e Matemática, Universidade do Recife, 1959. MR 24 #A3566 Zbl 0099.37402

[Hirsch 1994] M. W. Hirsch, *Differential topology*, Graduate Texts in Mathematics **33**, Springer, New York, 1994. MR 96c:57001

[Hopf 1983] H. Hopf, *Differential geometry in the large*, Lecture Notes in Mathematics **1000**, Springer, Berlin, 1983. MR 85b:53001 Zbl 0526.53002

[Hsiang 1982] W.-y. Hsiang, "Generalized rotational hypersurfaces of constant mean curvature in the Euclidean spaces, I", *J. Differential Geom.* **17** (1982), 337–356. MR 84h:53009 Zbl 0493.53043

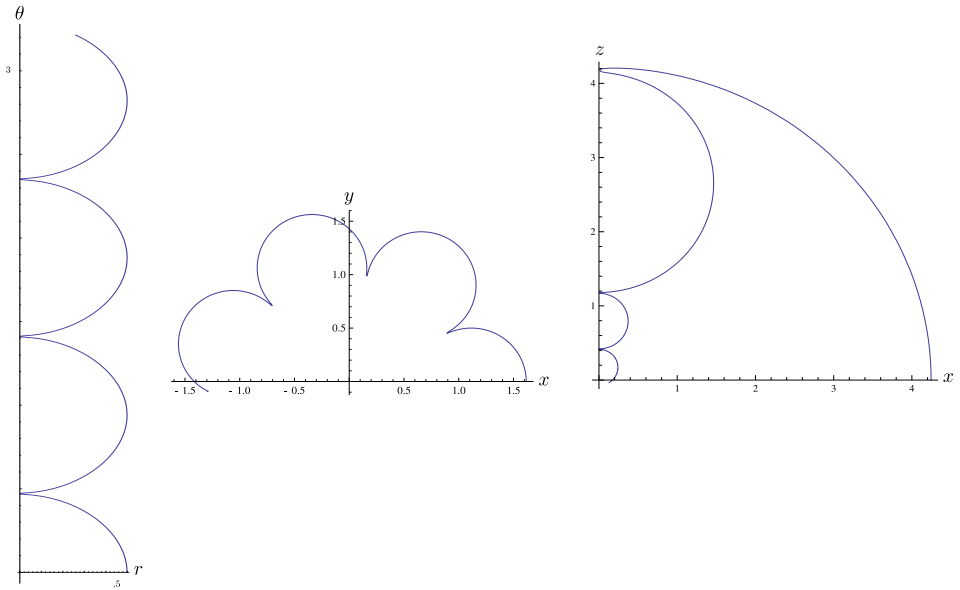

Figure 18. The generating curve of spheres, the stereographic projection of the curve $\phi = 0$ in Apollonian position, and the meridian of the same spheres in symmetric position. Note that the generating curve does not consist of arcs of circles, though the projection curves are arcs of circles.

[Hynd and McCuan 2006] R. Hynd and J. McCuan, "On toroidal rotating drops", *Pacific J. Math.* **224**:2 (2006), 279–289. MR 2007h:53010 Zbl 1125.49001

[Jagy 1998] W. C. Jagy, "Sphere-foliated constant mean curvature submanifolds", *Rocky Mountain J. Math.* **28**:3 (1998), 983–1015. MR 99j:53026 Zbl 0979.53072

[Kilian and Schmidt 2008] M. Kilian and M. U. Schmidt, "On the moduli of constant mean curvature cylinders of finite type in the 3-sphere", 2008. arXiv 0712.0108v2

[McCuan 1997] J. McCuan, "Symmetry via spherical reflection and spanning drops in a wedge", *Pacific J. Math.* **180**:2 (1997), 291–323. MR 98m:53013 Zbl 0885.53009

[McCuan and Spietz 1998] J. McCuan and L. Spietz, "Rotations of the three-sphere and symmetry of the Clifford torus", Mathematical Sciences Research Institute, 1998, Available at http://www.msri.org/publications/preprints/online/1998-052.html.

[Ôtsuki 1970] T. Ôtsuki, "Minimal hypersurfaces in a Riemannian manifold of constant curvature.", *Amer. J. Math.* **92** (1970), 145–173. MR 41 #9157 Zbl 0196.25102

[Otsuki 1988] T. Otsuki, "A nonlinear ordinary differential equation of order 2 in differential geometry", pp. 1001–1025 in *Topics in differential geometry, II* (Debrecen, 1984), edited by J. Szenthe and L. Tamássy, Colloq. Math. Soc. János Bolyai **46**, North-Holland, Amsterdam, 1988. MR 89g:53009 Zbl 0646.53054

[Park 2002] S.-H. Park, "Sphere-foliated minimal and constant mean curvature hypersurfaces in space forms and Lorentz–Minkowski space", *Rocky Mountain J. Math.* **32**:3 (2002), 1019–1044. MR 2003j:53037 Zbl 1043.53055

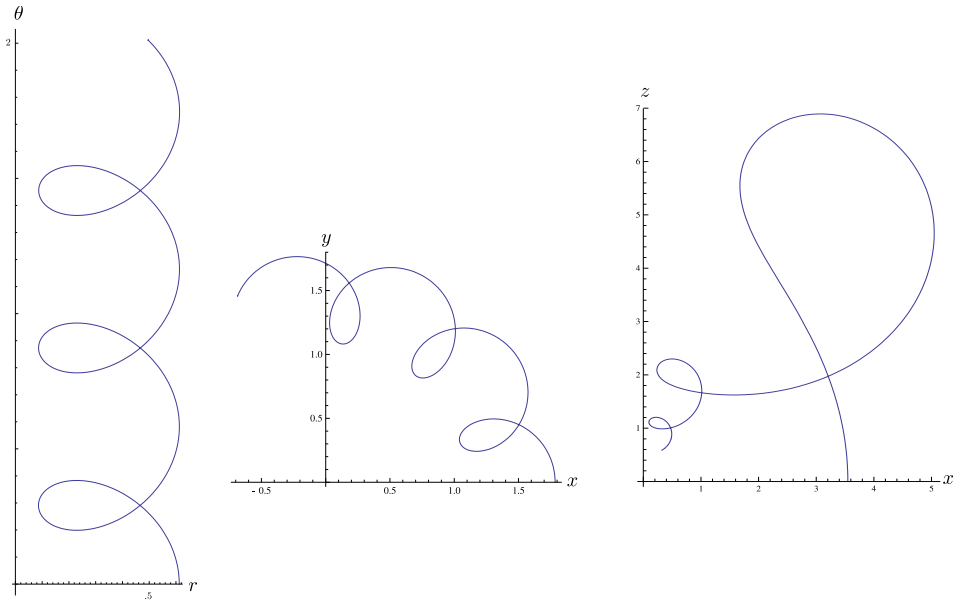

Figure 19. The generating curve of a nodoid-type surface, the stereographic projection of the curve $\phi = 0$ in Apollonian position, and the meridian of the same surface in symmetric position.

[Ros 1995] A. Ros, "A two-piece property for compact minimal surfaces in a three-sphere", *Indiana Univ. Math. J.* **44**:3 (1995), 841–849. MR 97g:53008 Zbl 0861.53009

[Rossman and Sultana 2007] W. Rossman and N. Sultana, "Morse index of constant mean curvature tori of revolution in the 3-sphere", *Illinois J. Math.* **51**:4 (2007), 1329–1340. MR 2417430

[Rossman and Sultana 2008] W. Rossman and N. Sultana, "The spectra of Jacobi operators for constant mean curvature tori of revolution in the 3-sphere", *Tokyo J. Math.* **31**:1 (2008), 161–174. MR 2009b:53010

[Wente 1980] H. C. Wente, "The symmetry of sessile and pendent drops", *Pacific J. Math.* **88**:2 (1980), 387–397. MR 83j:49042a Zbl 0473.76086

[Whittaker and Watson 1996] E. T. Whittaker and G. N. Watson, *A course of modern analysis: An introduction to the general theory of infinite processes and of analytic functions*, Cambridge University Press, 1996. MR 97k:01072 Zbl 0951.30002

[Yau 1982] S. T. Yau (editor), *Seminar on Differential Geometry*, Annals of Mathematics Studies **102**, Princeton University Press, 1982. MR 83a:53002

Received March 12, 2008. Revised January 19, 2009.

RYAN HYND
DEPARTMENT OF MATHEMATICS
UNIVERSITY OF CALIFORNIA
BERKELEY, CA 94720-3840
UNITED STATES
ryanhynd@math.berkeley.edu

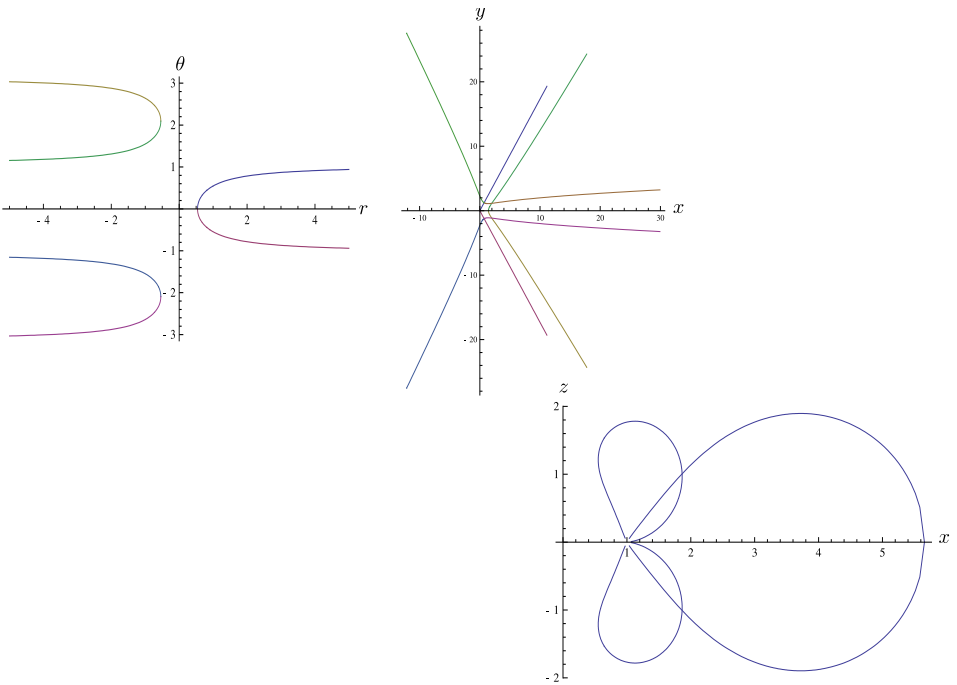

Figure 20. The generating curve of a catenoid-type surface, the stereographic projection of the curve $\phi = 0$ in Apollonian position, and the meridian of the same surface in symmetric position. This is the catenoid-type surface with $\theta_{\max} = \pi/3$, so the surface is compact. Three loops are shown in the meridian; there are three more, but it is not easy to guess how they will look. In contrast, the three missing from the $\phi = 0$ curve are easy to draw in.

SUNG-HO PARK
KIAS HOEGIRO
87(207-43 CHEONGNYANGNI 2-DONG)
DONGDAEMUN-GU
SEOUL 130-722
SOUTH KOREA
shubuti@kias.re.kr

JOHN MCCUAN
SCHOOL OF MATHEMATICS
GEORGIA TECH
686 CHERRY STREET
ATLANTA, GA 30332
UNITED STATES
mccuan@math.gatech.edu
http://www.math.gatech.edu/~mccuan